

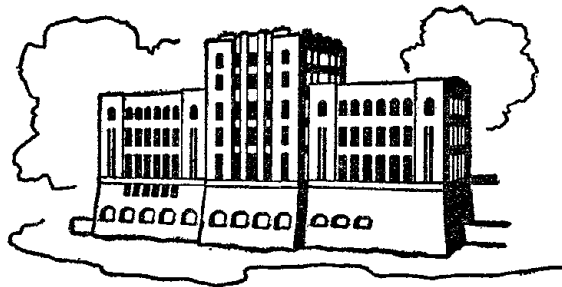
EARTHQUAKE EFFECTS ON RECTANGULAR DAM-RESERVOIR SYSTEMS

by

T. H. Huang and Allen T. Chwang

Sponsored by

National Science Foundation
Grant PFR 77-16085

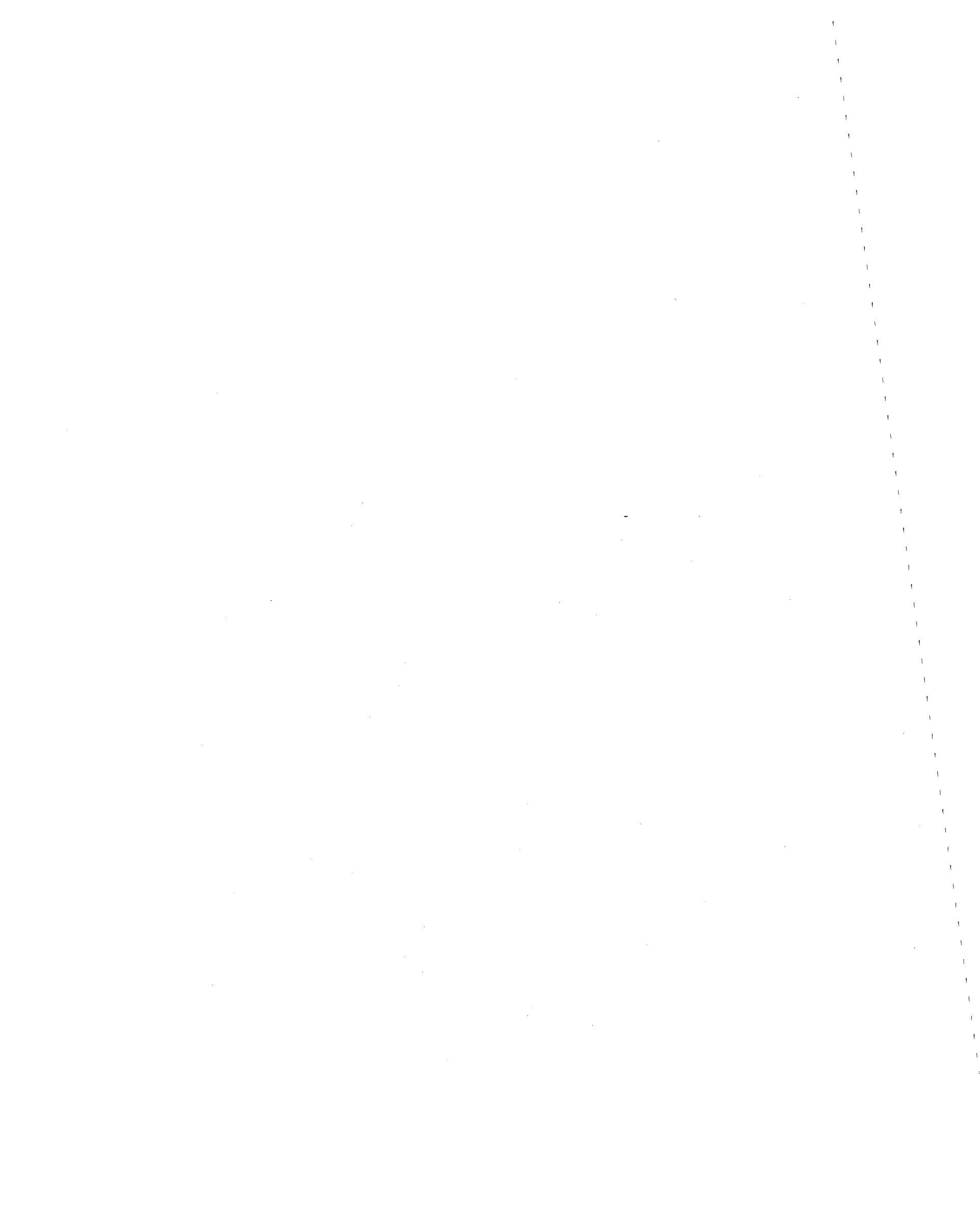


IIHR Report No. 245

Iowa Institute of Hydraulic Research
The University of Iowa
Iowa City, Iowa 52242

July 1982

REPRODUCED BY
NATIONAL TECHNICAL
INFORMATION SERVICE
U.S. DEPARTMENT OF COMMERCE
SPRINGFIELD, VA. 22161



EARTHQUAKE EFFECTS ON RECTANGULAR DAM-RESERVOIR SYSTEMS

by

T. H. Huang and Allen T. Chwang

Sponsored by

National Science Foundation
Grant PFR 77-16085

IIHR Report No. 245

Iowa Institute of Hydraulic Research
The University of Iowa
Iowa City, Iowa 52242

July 1982



ABSTRACT

This report represents essentially the thesis submitted by T.H. Huang in partial fulfillment of the requirements for the degree of Master of Science in Mechanical Engineering at The University of Iowa. Professor Allen T. Chwang was supervisor of the research project and thesis advisor.

This study deals with the earthquake effect on a three-dimensional, rectangular dam-reservoir system with vertical boundary. Both the longitudinal and the lateral harmonic ground excitations have been investigated. The compressibility of water, the seismic wave attenuation and the phase difference between two ends of a reservoir are considered. Analytic solutions are obtained for the hydrodynamic pressures, forces, and moments by using the method of orthogonal expansions. The possibility of resonance is discussed. Resonances tend to occur for a deep dam excited by a ground motion of small seismic period. The effects of the seismic wave attenuation, the phase difference, and the length of a reservoir are found to be small.

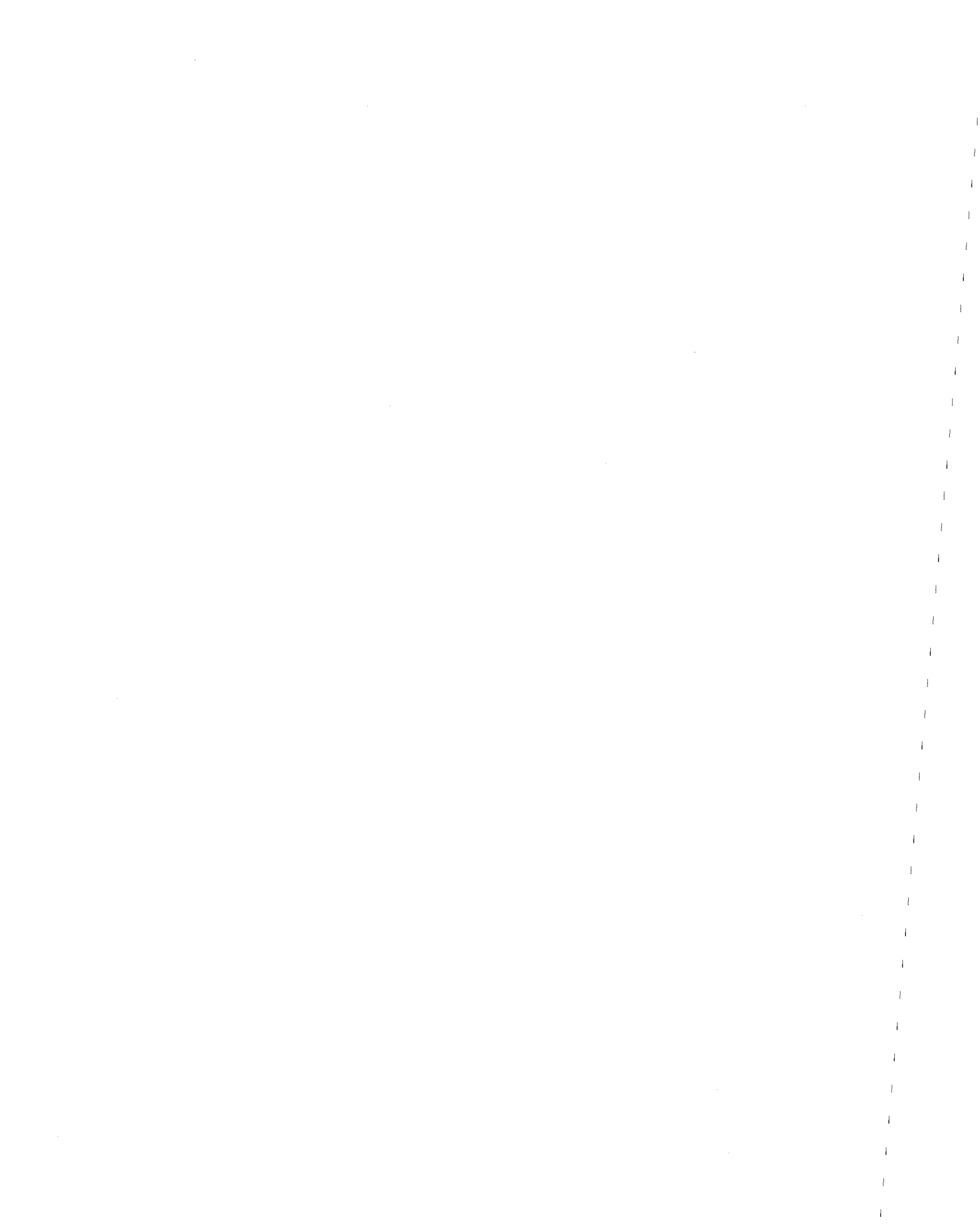


TABLE OF CONTENTS

LIST OF FIGURES	iii
LIST OF SYMBOLS	v
I. INTRODUCTION	1
1.1 Review of Pertinent Literature	1
1.2 Assumptions	3
II. RESPONSE TO LONGITUDINAL EXCITATIONS	6
2.1 Governing Equations and Corresponding Solutions	6
2.2 Pressure Distribution on Dams	9
2.3 Hydrodynamic Forces and Moments	11
2.4 Discussion of Results	13
III. RESPONSE TO LATERAL EXCITATIONS	20
3.1 Governing Equations and Corresponding Solutions	20
3.2 Pressure Distribution on Dams	21
3.3 Hydrodynamic Forces and Moments	22
3.4 Discussion of Results	24
IV. CONCLUSIONS	27
REFERENCES	30

LIST OF FIGURES

Figure		Page
1.	A Schematic Diagram of a Rectangular Dam-Reservoir System. (a) Side View, (b) Top View, (c) x'y'z' Coordinate System.	31
2.	Variation of the Hydrodynamic Force Coefficient with the Length-to-Depth Ratio ℓ/H due to a Longitudinal Excitation at $\beta = 1.0$ and $\omega H/c = 0.0$.	33
3.	Variation of the Hydrodynamic Moment Coefficient with the Length-to-Depth Ratio ℓ/H due to a Longitudinal Excitation at $\beta = 1.0$ and $\omega H/c = 0.0$.	34
4.	Variation of the Hydrodynamic Pressure Coefficient with the Length-to-Depth Ratio ℓ/H due to a Longitudinal Excitation at $\beta = 1.0$, $\omega H/c = 0.0$, $\alpha = 0$, and $\alpha = \pi$.	35
5.	Variation of the Hydrodynamic Pressure Coefficient with the Length-to-Depth Ratio ℓ/H due to a Longitudinal Excitation at $\beta = 1.0$, $\omega H/c = 0.0$, and $\alpha = \pi/4$. (a) In-Phase Component C_{pi} , (b) Out-of-Phase Component C_{po} , (c) Total Hydrodynamic Pressure Coefficient C_p .	36
6.	Variation of the Hydrodynamic Pressure Coefficient with the Length-to-Depth Ratio ℓ/H due to a Longitudinal Excitation at $\beta = 1.0$, $\omega H/c = 0.0$, and $\alpha = \pi/2$.	38
7.	Variation of the Hydrodynamic Force Coefficient with the Compressibility Parameter $\omega H/c$ due to a Longitudinal Excitation at $\beta = 1.0$, $\ell/H = 10.0$, $\alpha = 0$, and $\alpha = \pi$.	39

Figure		Page
8.	Variation of the Hydrodynamic Moment Coefficient with the Compressibility Parameter $\omega H/c$ due to a Longitudinal Excitation at $\beta = 1.0$, $\ell/H = 10.0$, $\alpha = 0$, and $\alpha = \pi$.	40
9.	Variation of the Hydrodynamic Pressure Coefficient with the Compressibility Parameter $\omega H/c$ due to a Longitudinal Excitation at $\beta = 1.0$, $\ell/H = 10.0$, $\alpha = 0$, and $\alpha = \pi$.	41
10.	Variation of the Hydrodynamic Force and Moment Coefficients with the Attenuation Factor β due to a Longitudinal Excitation at $\omega H/c = 0.0$, $\ell/H = 1.0$, and $\ell/H = 10.0$.	42
11.	Variation of the Hydrodynamic Pressure, Force, and Moment Coefficients with the Phase-Shift Angle α due to a Longitudinal Excitation at $\beta = 1.0$, $\omega H/c = 0.0$, $\ell/H = 1.0$, and $\ell/H = 10.0$.	43
12.	Variation of the Hydrodynamic Pressure Coefficient with the Width-to-Depth Ratio y/H due to a Lateral Excitation at $\omega H/c = 0.0$ and $b/H = 2.0$.	44
13.	Variation of the Hydrodynamic Force Coefficient with the Compressibility Parameter $\omega H/c$ due to a Lateral Excitation at $b/H = 2.0$ and $a/b = 1.0$.	45
14.	Variation of the Hydrodynamic Moment Coefficient with the Compressibility Parameter $\omega H/c$ due to a Lateral Excitation at $b/H = 2.0$ and $a/b = 1.0$.	46
15.	Variation of the Hydrodynamic Pressure Coefficient with the Compressibility Parameter $\omega H/c$ due to a Lateral Excitation at $b/H = 2.0$, $a/b = 1.0$, and $y/H = -1.0$.	47

LIST OF SYMBOLS

a	width of dam
b	width of reservoir
b^*	b/H
C_o	phase velocity of seismic wave
C_f	total hydrodynamic force coefficient due to a longitudinal excitation
C_{fi}	in-phase component of hydrodynamic force coefficient due to a longitudinal excitation
C_{fo}	out-of-phase component of hydrodynamic force coefficient due to a longitudinal excitation
C_f'	hydrodynamic force coefficient due to a lateral excitation
C_p	total hydrodynamic pressure coefficient due to a longitudinal excitation
C_{pi}	in-phase component of hydrodynamic pressure coefficient due to a longitudinal excitation
C_{po}	out-of-phase component of hydrodynamic pressure coefficient due to a longitudinal excitation
C_p'	hydrodynamic pressure coefficient due to a lateral excitation
C_m	total hydrodynamic moment coefficient due to a longitudinal excitation

C_{mi}	in-phase component of hydrodynamic moment coefficient due to a longitudinal excitation
C_{mo}	out-of-phase component of hydrodynamic moment coefficient due to a longitudinal excitation
C_m'	hydrodynamic moment coefficient due to a lateral excitation
C^*	$\omega H/c$; compressibility factor
C_{mn}^*	C^* at resonant mode mn
c	speed of sound in water
E	peak elastic energy in a certain volume
ΔE	amount of energy dissipated per cycle of a harmonic excitation in a certain volume
E_n	$H \cdot \mu_n$
F	total hydrodynamic force on a dam due to a longitudinal excitation
F'	total hydrodynamic force on a dam due to a lateral excitation
f'	hydrodynamic force per unit width due to a lateral excitation
H	depth of a dam-reservoir system
l	length of a dam-reservoir system
l^*	l/H
M	total hydrodynamic moment with respect to the base of a dam due to a longitudinal excitation

m'	hydrodynamic moment per unit width with respect to the base of a dam due to a lateral excitation
N	the largest integer such that the inequality $(n-1/2)\pi \leq \omega H/c$ is held
n^*	$(2n-1)\pi/2$
P	hydrodynamic pressure due to a longitudinal excitation
P'	hydrodynamic pressure due to a lateral excitation
Q	$2\pi E/\Delta E$; a measure of attenuation
r	distance from epicenter
T	period of ground motion
t	time
\vec{V}	velocity vector
y'	$y+b/2$
y^*	y/H
z^*	z/H
ω	frequency of ground motion
ω_{mn}	resonant frequency
α	phase difference between a dam and the distal end of a reservoir
α_0	$\omega/(2C_0 Q)$
β	ratio of the magnitude of a seismic wave at $x=l$ to that at $x=0$
β_0	spatial attenuation factor for a seismic wave

ϕ	velocity potential due to a longitudinal excitation
ϕ'	velocity potential due to a lateral excitation
ρ	density of water
σ_n	$\sqrt{(\omega/c)^2 - \lambda_n^2}$
λ_n	$(2n-1)\pi/2H$
u_n	$ \sigma_n $

I. INTRODUCTION

1.1 Review of Pertinent Literature

In view of the catastrophic consequences of dam failure, the investigation of the earthquake effect on a dam-reservoir system is particularly important. A large volume of literature concerned with water pressures on rigid dams during earthquakes has been published in the recent decades.

Westergaard (1933) first derived an expression for the hydrodynamic pressure exerted on a rigid dam with vertical upstream face by an incompressible fluid in a reservoir. The "added mass" theory was presented in his paper by ignoring the effect of surface waves and by assuming that the reservoir is infinitely long.

Based on his experimental results, Zangar (1953) concluded that the hydrodynamic pressure on a dam with the upstream face vertical for half or more of the total height will practically be the same as that of a fully vertical dam. Also, by ignoring the compressibility of water, Werner and Sundquist (1949) produced a solution for an incompressible fluid in a reservoir of finite length with two ends of the reservoir moving in phase or 180° out of phase. They

concluded that the motion of the distal end of the reservoir is immaterial if its amplitude does not exceed that of the motion of the dam site and provided that the ratio of the length of a reservoir to its depth is not smaller than 3. Moreover, in 1949, they found that the compressibility of water may play an important role in determining the hydrodynamic pressure on a dam and that resonances, which depend on the length of the reservoir, may occur. Kotsubo (1959) has shown that Westergaard's solution is valid only when the period of a harmonic excitation is greater than the fundamental natural period of a reservoir. Chopra (1967) also presented a complex frequency response and a unit impulse response of a vertical dam to a horizontal ground acceleration with a compressible fluid kept in a reservoir of infinite length. He demonstrated that the errors introduced by neglecting the compressibility of water could be 20% for a reservoir with a depth of 100 ft. and may be up to 51% for a 600 ft. deep reservoir. Thus, as we shall see later, the motion of the distal end of the dam would not be immaterial if the fluid were compressible. However, the surface wave effect on the hydrodynamic pressure will be neglected in this thesis.

1.2 Assumptions

We propose to analyze the hydrodynamic pressure of a three-dimensional dam-reservoir system. The dam-reservoir system, like many other gravity dam-reservoir systems in the United States such as Henshaw Dam in San Diego, Tygart Dam in West Virginia, Kensico Dam in New York or City Reservoir No. 3 Dam in Portland, Oregon, may be simplified as a rectangular reservoir of constant depth with the dam located at one end. The dam and the reservoir are assumed to be rigid. The hydrodynamic pressure on the vertical upstream face of the dam would be the real part of the response to the complex acceleration $e^{i\omega t}$. This investigation will contain two parts; one is that the system moves longitudinally along the extending direction of the reservoir and the other is that the excitation is parallel to the upstream face of the dam in the horizontal direction. Under the assumption of the linearity of this problem, the solution due to arbitrary horizontal excitations can be obtained by superposing the results of these two cases.

The period of a ground excitation during a typical earthquake may range from 0.1 to 10 seconds; and the shear wave speed on the ground usually varies from 1,000 ft/sec for soft soil to 10,000 ft/sec for hard rocks. If

we assume the period to be 0.5 second and the wave speed to be 5,000 ft/sec, then the wave length of the shear waves caused by an earthquake is about 2,500 ft which is of the same order of magnitude as the dimensions of a common dam-reservoir system. If a reservoir is 1.5 miles long, the ground acceleration at the dam will be about 6π radians out of phase comparing with that at the distal end of the reservoir. Therefore, the phase differences must be taken into account to set up the boundary conditions at the dam and along the side boundaries of the reservoir. In addition, the amplitude of seismic waves decreases with distance. For a reliable estimate, we may adopt the formula

$$\beta_0 = r^{-n} e^{-\alpha_0 r} \quad (1)$$

as the spatial attenuation factor for a wave function as discussed in detail by Press (1964) and Knopoff (1964). In Equation (1), r is the distance from the epicenter, n is a constant, and α_0 is related to the dimensionless quality factor Q by (Knopoff, 1964)

$$\alpha_0 = \omega / (2C_0 Q), \quad (2a)$$

where ω is the frequency and C_0 the phase velocity of a

seismic wave. The dimensionless quality factor Q , which is a measure of attenuation, is defined by

$$Q = 2\pi E/\Delta E, \quad (2b)$$

where ΔE is the amount of energy dissipated per cycle of a harmonic excitation in a certain volume, and E is the peak elastic energy in the system in the same volume.

We also assume that the amplitude of the excitation is small, the fluid is compressible and inviscid and the flow irrotational. By ignoring the convective effects, we can derive a governing wave equation for the velocity potential in view of the linearity of our problem. The free surface is assumed to be fixed so that no surface waves exist. By the method of orthogonal expansions, analytic solutions can be found. In this thesis, influence factors such as the phase difference, the spatial attenuation factor, the compressibility of the water, and the dimensions of the dam-reservoir system, as well as the resonance phenomenon will be discussed in detail with clear presentation by graphs for both the longitudinal and the lateral ground excitations.

II. RESPONSE TO LONGITUDINAL EXCITATIONS

2.1 Governing Equations and Corresponding Solutions

The geometric shape of the reservoir of a dam-reservoir system is assumed to be rectangular. Let the x-axis be the direction perpendicular to the upstream face of the dam, lying in the horizontal ground plane and passing through the center of the base of the dam (see Figures 1a and 1b). The y-axis is in the horizontal plane perpendicular to the x-axis, and the z-axis is pointing upwards in the vertical direction. Let the bottom of the reservoir be at $z=0$, and the water depth be H . The reservoir is bounded in the x direction by $x=0$ and $x=l$, in the y direction by $y=-b/2$ and $y=b/2$. The dam spans from $y=-a/2$ to $y=a/2$ at $x=0$. We shall investigate the hydrodynamic response of this dam-reservoir system due to a longitudinal harmonic ground excitation. We shall assume that the ground acceleration is in the x direction with a magnitude of $e^{i\omega t}$ at $x=0$ and $\beta e^{i(\omega t + \alpha)}$ at $x=l$, where α is a constant phase difference and β , which is assumed to be a constant, is the ratio of the magnitude of the ground acceleration at $x=l$ to that at $x=0$ representing the attenuation effect of seismic waves.

If we neglect the effects of viscosity of water and assume that the amplitudes of water motion are small, the motion of the water is governed by the wave equation,

$$\frac{\partial^2 \phi}{\partial x^2} + \frac{\partial^2 \phi}{\partial y^2} + \frac{\partial^2 \phi}{\partial z^2} = \frac{1}{c^2} \frac{\partial^2 \phi}{\partial t^2}, \quad (3)$$

where $\phi(x, y, z, t)$ is the velocity potential which is defined as $\nabla\phi = \vec{V}$ with \vec{V} being the velocity vector. Here c is the speed of sound in water given by

$$c^2 = \left(\frac{dP}{d\rho}\right)_s, \quad (4)$$

where P is the thermodynamic pressure, ρ is the density of water and s means that the differentiation is evaluated at constant entropy. The hydrodynamic pressure $P(x, y, z, t)$ is related to ϕ by

$$P = -\rho \frac{\partial \phi}{\partial t}. \quad (5)$$

The boundary conditions are as follows:

$$\phi_x(0, y, z, t) = -\frac{i}{\omega} e^{i\omega t}, \quad (6a)$$

$$\phi_x(l, y, z, t) = -\frac{i\beta}{\omega} e^{i(\omega t + \alpha)}, \quad (6b)$$

$$\phi_{,y}(x, \pm b/2, z, t) = 0, \quad (6c)$$

$$\phi_{,z}(x, y, 0, t) = 0, \quad (6d)$$

and

$$\phi_{,t}(x, y, H, t) = 0. \quad (6e)$$

By the method of separation of variables, the solution of equation (3) satisfying the boundary conditions (6a) to (6e) can be found as

$$\phi(x, y, z, t) = \frac{2i}{\omega H} \sum_{n=1}^{\infty} (-1)^n \frac{\cos(\sigma_n(\ell-x)) - \beta e^{i\alpha} \cos(\sigma_n x)}{\sigma_n \lambda_n \sin(\sigma_n \ell)} \cos(\lambda_n z) e^{i\omega t}, \quad (7)$$

where

$$\lambda_n = \frac{(2n-1)\pi}{2H} \quad (n=1, 2, 3, \dots), \quad (8)$$

and

$$\sigma_n = \sqrt{(\omega/c)^2 - \lambda_n^2} \quad (n=1, 2, 3, \dots), \quad (9)$$

where the positive branch is taken for the square-root function. Depending on the relative magnitude of ω/c and λ_n , σ_n may

be imaginary. It should be noted that the velocity potential ϕ given by (7) is independent of y because of the symmetry of the motion and that of the reservoir.

2.2 Pressure Distribution on Dams

The hydrodynamic pressure on the vertical upstream face of a dam is the real part of $-\rho \frac{\partial \phi}{\partial t}$ at $x=0$. Therefore,

$$P(0, y, z, t) = \frac{2\rho}{H} \sum_{n=1}^{\infty} \frac{(-1)^{n+1} \cos(\lambda_n z)}{\sigma_n \lambda_n \sin(\sigma_n \ell)} \{ (\beta \cos \alpha - \cos(\sigma_n \ell)) \cdot \cos(\omega t) - \beta \sin \alpha \sin(\omega t) \}, \quad (10)$$

or

$$P(0, y, z, t) = \frac{2\rho}{H} \sum_{n=1}^N \frac{(-1)^{n+1} \cos(\lambda_n z)}{\mu_n \lambda_n \sin(\mu_n \ell)} \{ (\beta \cos \alpha - \cos(\mu_n \ell)) \cdot \cos(\omega t) - \beta \sin \alpha \sin(\omega t) \} +$$

$$\frac{2\rho}{H} \sum_{n=N+1}^{\infty} \frac{(-1)^n \cos(\lambda_n z)}{\mu_n \lambda_n \sinh(\mu_n \ell)} \{ (\beta \cos \alpha - \cosh(\mu_n \ell)) \cdot \cos(\omega t) - \beta \sin \alpha \sin(\omega t) \}, \quad (11)$$

where $\mu_n = |\sigma_n|$ ($n=1,2,3,\dots$), and for fixed ω and c , N is the largest integer such that the inequality $(n-\frac{1}{2})\pi \leq \frac{\omega H}{c}$ is held. Therefore, for $n \leq N$, $\mu_n = \sigma_n$; for $n > N$, $\mu_n = -i\sigma_n$.

Let the hydrodynamic pressure coefficients C_{pi} and C_{po} be defined as

$$\frac{P(0,y,z,t)}{\rho H} = C_{pi} \cos(\omega t) + C_{po} \sin(\omega t), \quad (12)$$

where C_{pi} and C_{po} denote the in-phase and out-of-phase pressure coefficients, respectively. Therefore,

$$C_{pi} = \sum_{n=1}^{\infty} \frac{2(-1)^{n+1} \cos(\lambda_n z) (\beta \cos \alpha - \cos(\sigma_n \ell))}{\sigma_n H^2 \lambda_n \sin(\sigma_n \ell)} \quad (13a)$$

and

$$C_{po} = \sum_{n=1}^{\infty} \frac{2(-1)^n \cos(\lambda_n z) \beta \sin \alpha}{\sigma_n H^2 \lambda_n \sin(\sigma_n \ell)}. \quad (13b)$$

If we let $n^* = (2n-1)\pi/2$, $C^* = \omega H/c$, $\ell^* = \ell/H$, $b^* = b/H$, $z^* = z/H$, and $E_n = H \cdot \mu_n$, then

$$C_{pi} = \sum_{n=1}^N (-1)^{n+1} \frac{2 \cos(n^* z^*)}{n^* E_n} \cdot \frac{\beta \cos \alpha - \cos(E_n \cdot \ell^*)}{\sin(E_n \cdot \ell^*)} + \sum_{n=N+1}^{\infty} (-1)^n \frac{2 \cos(n^* z^*)}{n^* E_n} \cdot \frac{\beta \cos \alpha - \cosh(E_n \cdot \ell^*)}{\sinh(E_n \cdot \ell^*)}, \quad (13c)$$

and

$$C_{po} = \sum_{n=1}^N (-1)^n \frac{2\cos(n^*z^*)}{n^*E_n} \cdot \frac{\beta \sin \alpha}{\sin(E_n \cdot \ell^*)} + \sum_{n=N+1}^{\infty} (-1)^{n+1} \frac{2\cos(n^*z^*)}{n^*E_n} \cdot \frac{\beta \sin \alpha}{\sinh(E_n \cdot \ell^*)} \quad (13d)$$

These two coefficients are non-dimensional.

2.3 Hydrodynamic Forces and Moments

The total hydrodynamic force $F(t)$ on the upstream face of a dam can be calculated by integrating the hydrodynamic pressure over the upstream area of the dam. Thus,

$$\begin{aligned} F(t) &= \int_{-a/2}^{a/2} dy \int_0^H P(0, y, z, t) dz \\ &= \frac{2\rho a}{H} \sum_{n=1}^{\infty} \frac{(\beta \cos \alpha - \cos(\sigma_n \ell)) \cos(\omega t) - \beta \sin \alpha \sin(\omega t)}{\sigma_n \lambda_n^2 \sin(\sigma_n \ell)} \end{aligned} \quad (14)$$

If we define the hydrodynamic force coefficients C_{fi} and C_{fo} as

$$\frac{F(t)}{\rho \cdot a \cdot H^2} = C_{fi} \cos(\omega t) + C_{fo} \sin(\omega t) \quad , \quad (15)$$

where the suffices i and o denote the in-phase and out-of-phase components respectively. Then,

$$C_{fi} = \sum_{n=1}^{\infty} \frac{2(\beta \cos \alpha - \cos(\sigma_n \ell))}{H^3 \sigma_n \lambda_n^2 \sin(\sigma_n \ell)}, \quad (16a)$$

and

$$C_{fo} = \sum_{n=1}^{\infty} \frac{-2\beta \sin \alpha}{H^3 \sigma_n \lambda_n^2 \sin(\sigma_n \ell)}. \quad (16b)$$

Applying the same notations as in (13c) and (13d), we have

$$C_{fi} = \sum_{n=1}^N \frac{2(\beta \cos \alpha - \cos(E_n \cdot \ell^*))}{n^2 E_n \sin(E_n \cdot \ell^*)} - \sum_{n=N+1}^{\infty} \frac{2(\beta \cos \alpha - \cosh(E_n \cdot \ell^*))}{n^2 E_n \sinh(E_n \cdot \ell^*)}, \quad (16c)$$

and

$$C_{fo} = \sum_{n=1}^N \frac{-2\beta \sin \alpha}{n^2 E_n \sin(E_n \cdot \ell^*)} + \sum_{n=N+1}^{\infty} \frac{2\beta \sin \alpha}{n^2 E_n \sinh(E_n \cdot \ell^*)}. \quad (16d)$$

The total hydrodynamic moment with respect to the base of the dam, $M(t)$, can be found as

$$\begin{aligned} M(t) &= \int_{-a/2}^{a/2} dy \int_0^H P(0, y, z, t) \cdot z dz \\ &= \rho a H^3 (C_{mi} \cos(\omega t) + C_{mo} \sin(\omega t)), \end{aligned} \quad (17)$$

where the hydrodynamic moment coefficients are given by

$$C_{mi} = \sum_{n=1}^N \frac{2(n^* + (-1)^n)(\beta \cos \alpha - \cos(E_n \cdot \ell^*))}{n^{*3} E_n \sin(E_n \cdot \ell^*)} - \sum_{n=N+1}^{\infty} \frac{2(n^* + (-1)^n)(\beta \cos \alpha - \cosh(E_n \cdot \ell^*))}{n^{*3} E_n \sinh(E_n \cdot \ell^*)}, \quad (18a)$$

and

$$C_{mo} = \sum_{n=1}^N \frac{-2(n^* + (-1)^n) \beta \sin \alpha}{n^{*3} E_n \sin(E_n \cdot \ell^*)} + \sum_{n=N+1}^{\infty} \frac{2(n^* + (-1)^n) \beta \sin \alpha}{n^{*3} E_n \sinh(E_n \cdot \ell^*)}. \quad (18b)$$

2.4 Discussion of Results

For an incompressible fluid in an infinitely long reservoir ($c \rightarrow \infty$, $\ell \rightarrow \infty$, and $\alpha = 0$), the velocity potential given by (7) reduces to

$$\phi(x, z, t) = \frac{2i}{\omega H} \sum_{n=1}^{\infty} (-1)^{n+1} \frac{\cos(\lambda_n z) e^{-\lambda_n x} e^{i\omega t}}{\lambda_n^2}, \quad (19)$$

which is the same as that given by Westergaard (1933). The corresponding hydrodynamic pressure coefficients, force coefficients and moment coefficients become

$$C_{pi} = 2 \sum_{n=1}^{\infty} \frac{(-1)^{n+1}}{n^{*2}} \cos(n^*z^*) , C_{po}(z^*) = 0 , \quad (20a)$$

$$C_{fi} = 2 \sum_{n=1}^{\infty} (n^*)^{-3} , C_{fo} = 0 , \quad (20b)$$

$$C_{mi} = 2 \sum_{n=1}^{\infty} \frac{(-1)^n + n^*}{n^{*4}} , C_{mo} = 0 . \quad (20c)$$

For an incompressible fluid in a finite reservoir when the end walls (at $x=0$ and at $x=l$) move in phase without attenuation ($c \rightarrow \infty$, $\beta=1$, $\alpha=0$), the velocity potential given by (7) reduces to

$$\phi(x,z,t) = \frac{2i}{\omega H} \sum_{n=1}^{\infty} (-1)^{n+1} \frac{\cosh(\lambda_n(l-x)) - \cosh(\lambda_n x)}{\lambda_n^2 \sinh(\lambda_n l)} \cos(\lambda_n z) e^{i\omega t} . \quad (21a)$$

The corresponding pressure coefficients become

$$C_{pi} = 2 \sum_{n=1}^{\infty} (-1)^{n+1} \frac{\cosh(\lambda_n l) - 1}{\lambda_n^2 H^2 \sinh(\lambda_n l)} \cos(\lambda_n z) , \quad (21b)$$

$$C_{po} = 0 , \quad (21c)$$

which agree exactly with the results obtained by Werner and Sundquist (1949).

From Equations (13), (16) and (18), we note that the hydrodynamic pressure coefficients, force coefficients and

moment coefficients are independent of time. They are functions of nondimensional parameters λ^* , C^* , α , and β . we shall discuss the influence of these parameters in the following section. First of all, we shall define the total hydrodynamic pressure coefficient C_p as $C_p = \sqrt{C_{pi}^2 + C_{po}^2}$. Similarly, C_f and C_m can be defined. Obviously, these coefficients are more useful since they represent the maximum amplitudes.

The effect of λ^* ($\lambda^* = \lambda/H$) on the total force coefficients can be comprehended by examining its effect on the components C_{fo} and C_{fi} . C_{fo} is proportional to $\beta \sin \alpha$. This out-of-phase component becomes small as the length of the reservoir becomes large. Thus its magnitude decreases monotonically from infinity at $\lambda^*=0$ to zero as $\lambda^* \rightarrow \infty$. Its contribution to C_f is not negligible. C_{fi} contains two infinite series, namely

$$\sum_{n=N+1}^{\infty} \frac{2}{E_n n^{*2}} \frac{\cosh(E_n \lambda^*)}{\sinh(E_n \lambda^*)}, \quad (22a)$$

and

$$\sum_{n=N+1}^{\infty} \frac{-2}{E_n n^{*2}} \frac{\beta \cos \alpha}{\sinh(E_n \lambda^*)}. \quad (22b)$$

The former represents the force when the distal end of the reservoir is motionless. Therefore, it decreases

monotonically from infinity at $\ell^*=0$ to a finite value (0.542 for $\epsilon^*=0$) as $\ell^*\rightarrow\infty$. Since the longer the reservoir length the smaller the magnitude of the latter series will be, the latter series increases monotonically from $-\infty$ at $\ell^*=0$ to 0 as $\ell^*\rightarrow\infty$ when $\cos\alpha$ is positive. This negative contribution may cause C_{fi} , consequently C_f , to decrease first and then to increase as ℓ^* increases. This can clearly be seen in Fig. 2. For $\cos\alpha > 0$, the critical value of ℓ^* at which C_f is a minimum can usually be estimated by taking the derivative of the first term of the infinite series (22a) to be zero since the first term dominates the value of C_f if resonances do not occur. This ℓ^* is not greater than 3 in most cases. In case of $\cos\alpha < 0$, C_f would approach infinity as $\ell^*\rightarrow 0$ and would decrease monotonically as ℓ^* increases. However, the hydrodynamic force coefficient will increase as ℓ^* increases for $\beta\cos\alpha = 1$. The value of C_f approaches to 0.542 as $\ell^*\rightarrow\infty$ when the fluid is incompressible. This is the same value as that given by Chwang (1978). The influence of ℓ^* on the hydrodynamic force coefficient is less than 2% if ℓ^* is greater than 3. We note that most of the dam-reservoir systems do have values of ℓ^* greater than 3. For example, the Coralville Dam near Iowa City, Iowa, which keeps at an average 57 ft. elevation and spans about 0.5 mile long (idealized), has a value of ℓ^* around 46.

The influence of λ^* on the hydrodynamic moment coefficients and pressure coefficients is similar to that on force coefficients. The limiting value of C_m is 0.217 as $\lambda^* \rightarrow \infty$ for an incompressible fluid. This can be seen in Figure 3. Pressure distributions for $\alpha=0$, $\pi/4$, $\pi/2$, and π are shown in Figures 4, 5a, 5b, 5c, and 6. From these figures, we note that C_p is zero at the water surface, i.e., at $z=H$. The distributions increase smoothly with depth and the pressure is maximum at the base of the dam. As α equals zero or π , C_{po} vanishes and thus $C_p = C_{pi}$. And C_p approaches to 0.742 for any α and β at the base of the dam.

The influence of C^* on the force coefficient C_f is shown in Figure 7. Since the period of most seismic waves lies in the range of 0.1 sec to 10.0 sec, the depth H is about 100 ft to 1000 ft, and the speed of sound in water is 4720 ft/sec, C^* lies in the range of 0.01 to 14.0. C^* is a measure of the compressibility of the fluid. Figure 7 shows that C_f increases moderately with C^* if $0 \leq C^* < 1.5$ ($0 \leq H/T < 343$ m/sec); and it increases more rapidly as C^* approaches to $\pi/2$ ($H/T \rightarrow 360$ m/sec). If $C^* \geq \pi/2$, resonances occur. It also means that resonances will not happen if the seismic frequency does not exceed the fundamental natural frequency of the dam-reservoir system, that is $C^* < \lambda_1 H = \pi/2$, where λ_1 is the first eigenvalue of the reservoir. High

seismic frequency and large depth are apt to the occurrence of resonances.

The values of C_f at resonances are theoretically infinity. From equation (16), the $C_{\text{resonance}}^*$ is given by

$$C_{kn}^* = \frac{2k-1}{2}\pi \quad (k=1,2,3,\dots) \text{ for } \beta \cos \alpha \neq 1. \quad (23)$$

And this is also valid for $\beta \cos \alpha = 1$ if

$$l^* = m\pi (C^{*2} - n^{*2})^{-1/2},$$

where

$$m = 1, 3, 5, 7, \dots$$

Resonances also happen at

$$C_{kn}^* = \sqrt{\left(\frac{2k-1}{2}\pi\right)^2 + \left(\frac{n\pi}{l^*}\right)^2} \quad (k=1,2,3,\dots; n=1,2,3,\dots) \quad (24)$$

if $\beta \cos \alpha \neq 1$; or $\beta \cos \alpha = 1$, n is an odd integer; or $\beta \cos \alpha = -1$, n is an even integer. It is understandable that resonances occur alternately for $\alpha=0$ and $\alpha=\pi$ because of the effects of phase differences.

The influence of C^* on the hydrodynamic moment coefficient C_m is similar to that of C_f as shown in Figure 8. Figure 9 shows that there may be oscillations in the pressure distribution when $C^* > \pi/2$.

The effect of β on C_f and C_m can be quite different for different values of α . It is more sensitive if ℓ^* is smaller. Figure 10 shows the influence of β at $C^* = 0.0$ (incompressible) and $\ell^* = 1.0$. As β increases, C_f will increase if $\cos\alpha \leq 0$, but will decrease if $\cos\alpha > 0$. One reason for this is that the second part of the in-phase component (22b) contributes negatively to C_f (also C_m) for $\cos\alpha > 0$ and gives positive contribution for $\cos\alpha \leq 0$. Also, we can see from Figure 10 that C_f and C_m remain practically constant at $\ell^* = 10.0$. Since ℓ^* is normally greater than 3, the β influence is rather small for most dam-reservoir systems.

In Figure 11 we note that the effect of α on C_p (at $z=0$), C_f , and C_m is symmetric with respect to the line $\alpha=\pi$. Hydrodynamic pressures (or forces, moments) increase as α approaches to π and decrease as α tends to zero. They remain almost constant at $\ell^* = 10.0$. The effect of α is therefore small for most dam-reservoir systems.

III. RESPONSE TO LATERAL EXCITATIONS

3.1 Governing Equations and Corresponding Solutions

We shall adopt the same rectangular dam-reservoir system as described in Chapter II for the study of lateral excitations. For convenience, we select a new (x', y', z') coordinate system as shown in Figure 1c. This new (x', y', z') system is related to the previous system by

$$x'=x, \quad y'=y+b/2, \quad z'=z.$$

In most cases, the width of the dam is small in comparison with the length of the reservoir. If $b=200$ ft, the phase difference between two side boundaries for an excitation with 2500 ft wave length is about 0.15π . Therefore, we shall assume that the whole system moves with the same ground acceleration $e^{i\omega t}$. Hence, there is no terms of α and β involved in boundary conditions. Let $\phi'(x', y', z', t)$ denote the velocity potential of the reservoir. The superscript "'" denotes the y-direction excitation. The boundary conditions are

$$\phi'_{y'}(x', 0, z', t) = -\frac{i}{\omega} e^{i\omega t} , \quad (25a)$$

$$\phi'_{y'}(x', b, z', t) = -\frac{i}{\omega} e^{i\omega t} , \quad (25b)$$

$$\phi'_{z'}(x', y', 0, t) = 0 , \quad (25c)$$

and

$$\phi'_{t'}(x', y', H, t) = 0 . \quad (25d)$$

The solution of equation (3) satisfying the boundary conditions (25) is found to be

$$\phi' = \frac{2i}{\omega H} \sum_{n=1}^{\infty} (-1)^n \frac{\cos(\sigma_n(b-y')) - \cos(\sigma_n y')}{\sigma_n \lambda_n \sin(\sigma_n b)} \cos(\lambda_n z) e^{i\omega t} ,$$

where σ_n and λ_n are given by (9) and (8) respectively. Obviously, the velocity potential is independent of the length of the dam-reservoir system.

3.2 Pressure Distribution on Dams

The hydrodynamic pressure on the upstream face of the dam is the real part of $-\rho \frac{\partial \phi'}{\partial t}$ at $x=0$. Therefore,

$$P' = \frac{2\rho}{H} \sum_{n=1}^{\infty} (-1)^n \frac{\{\cos(\sigma_n(b-y')) - \cos(\sigma_n y')\}}{\sigma_n \lambda_n \sin(\sigma_n b)} \cdot \cos(\lambda_n z) \cos(\omega t) , \quad (26)$$

or

$$P' = C'_p (\rho H \cos(\omega t)) , \quad (27)$$

where the hydrodynamic pressure coefficient due to lateral excitation is given by

$$C'_p = \sum_{n=1}^N (-1)^n \frac{2\cos(n^* z^*)}{n^* \cdot E_n} \cdot \frac{\sin(E_n \cdot y^*)}{\cos(E_n \cdot b^*/2)} + \sum_{n=N+1}^{\infty} (-1)^n \frac{2\cos(n^* z^*)}{n^* \cdot E_n} \cdot \frac{\sinh(E_n \cdot y^*)}{\cosh(E_n \cdot b^*/2)} . \quad (28)$$

The dimensionless parameters n^* , z^* , b^* and E_n in equation (28) are given in equation (13), and y^* is defined by

$$y^* = y/H . \quad (29)$$

3.3 Hydrodynamic Forces and Moments

By integrating the hydrodynamic pressure P' over the depth of the dam, the hydrodynamic force per unit width $f'(y', t)$ at $x=0$ can be found as

$$\begin{aligned}
f'(y', t) &= \int_0^H P'(x', y', z, t) dz \\
&= \frac{2\rho}{H} \sum_{n=1}^{\infty} \frac{\cos(\sigma_n y') - \cos(\sigma_n (b-y'))}{\sigma_n \lambda_n^2 \sin(\sigma_n b)} \cos(\omega t). \quad (30)
\end{aligned}$$

The total hydrodynamic force $F'(t)$ is given by

$$F'(t) = \int_{(b-a)/2}^{(b+a)/2} f' \cdot dy' = 0. \quad (31a)$$

This means that the hydrodynamic force distribution along y' direction is anti-symmetric with respect to the plane $y' = b/2$ (or $y=0$). If we integrate f' from $y = -a/2$ ($y' = (b-a)/2$) to $y = 0$ ($y' = b/2$), then

$$\begin{aligned}
F'(t) &= \int_{(b-a)/2}^{b/2} f' \cdot dy' \\
&= \frac{4\rho}{H} \sum_{n=1}^{\infty} \frac{\sin(\sigma_n b/2) (1 - \cos(\sigma_n a/2))}{\sigma_n^2 \lambda_n^2 \sin(\sigma_n b)} \cos(\omega t). \quad (31b)
\end{aligned}$$

We define the hydrodynamic force coefficient by

$$C'_f = \frac{f'(y', t)}{\rho H^2 \cos(\omega t)}. \quad (32)$$

Therefore,

$$C'_f = - \sum_{n=1}^N \frac{2}{E_n \cdot n^2} \cdot \frac{\sin(E_n y^*)}{\cos(E_n b^*/2)} - \sum_{n=N+1}^{\infty} \frac{2}{E_n \cdot n^2} \cdot \frac{\sinh(E_n y^*)}{\cosh(E_n \cdot b^*/2)} \quad (33)$$

Also, the hydrodynamic moment per unit width with respect to the base of the dam is given by

$$m'(y', t) = \int_0^H z P' dz = C'_m \rho H^3 \cos(\omega t) \quad , \quad (34)$$

where

$$C'_m = \sum_{n=1}^N ((-1)^{n+1} - n^*) \cdot \frac{2}{E_n \cdot n^3} \cdot \frac{\sin(E_n y^*)}{\cos(E_n b^*/2)} + \sum_{n=N+1}^{\infty} ((-1)^{n+1} - n^*) \cdot \frac{2}{E_n \cdot n^3} \cdot \frac{\sinh(E_n \cdot y^*)}{\cosh(E_n \cdot b^*/2)} \quad (35)$$

3.4 Discussion of Results

The hydrodynamic pressure coefficient C'_p at several values of y^* is shown in Figure 12. We note that the magnitude of C'_p increases as y^* increases; and $C'_p = 0$ at the plane $y=0$. This trend, however, will break down if resonances take place. Resonant frequency can be found by letting

$$E_n b^*/2 = (2m-1)\pi/2 \quad (m=1,2,3,\dots) .$$

That is

$$C_{mn}^* = \sqrt{\left(\frac{(2n-1)\pi}{2}\right)^2 + \left(\frac{(2m-1)\pi}{b^*}\right)^2} \quad (n=1,2,3,\dots) . \quad (36)$$

From (36), if $b^* = 2.0$ and $c = 4720$ ft/sec, then the smallest C^* for resonance to occur is C_{11}^* which is about 2.22. The corresponding value of H/T for the system is

$$H/T \doteq 1668 \text{ ft/sec} \doteq 508 \text{ m/sec} . \quad (37)$$

Also from (36), we know that the resonant frequency ω_{mn} is given by

$$\omega_{mn}^2 = (\lambda_n c)^2 + \left(\frac{(2m-1)\pi}{b} \cdot c\right)^2 . \quad (38)$$

If the ground excitation frequency $\omega < \omega_{11}$, no resonance can happen. A high seismic frequency and large values of depth and width would more likely cause resonances. The hydrodynamic response to lateral excitations is anti-symmetric with respect to the $y=0$ plane. The first discontinuity of the curves in Figures 13 and 14 at $C_{11}^* = 2.22$ (at $b^* = 2.0$) is due to the first natural resonant frequency of the system. At second natural resonant frequency ($C_{21}^* = 4.97$), there

are some nodes of standing waves and thus the discontinuities of the curves are different for different values of y^* . Figure 15 shows that the hydrodynamic pressure distribution may be oscillatory when C^* becomes large.

IV. CONCLUSIONS

The present study has lead to the following conclusions for longitudinal earthquake excitations:

- (1) The hydrodynamic forces are not sensitive to l/H when l/H is greater than 3. Only relatively short reservoirs (i.e., $l/H < 3$), which are unusual among existing reservoirs, may be influenced considerably by l/H .
- (2) The occurrence of resonance depends on the ratio H/T . This ratio plays an important role in most failures of dams during earthquakes. A low-dam design tends to be on the safe side. Resonances will not take place if $H/T < 360$ m/sec.
- (3) At $\alpha=0$, the hydrodynamic force coefficient reaches a minimum and at $\alpha=\pi$ a maximum when $C^* < C_{11}^*$. And the influence of α on C_f is very small when $l/H > 3$. For $C^* > C_{11}^*$, resonances may occur. The resonant frequencies for $\alpha=0$ and $\alpha=\pi$ take place alternately with the increase of C^* .
- (4) The increase of β has positive contribution to the hydrodynamic force coefficient when $\cos\alpha \leq 0$

and negative contribution when $\cos\alpha > 0$. The overall effect of β is rather small for $\ell/H < 3$.

- (5) The pressure distribution increases monotonically with the depth. But if $C^* > C_{11}^*$, it may oscillate.

The study of lateral excitations leads to the following conclusions:

- (1) If $C^* < C_{11}^*$, the magnitude of the hydrodynamic pressure coefficient increases with an increase of y . For any C^* , the hydrodynamic pressure and force coefficients are anti-symmetric with respect to the plane $y=0$. They also oscillate along the y direction when C^* is closer to C_{11}^* . Thus, the bending of a dam should be considered in the design process.
- (2) Resonances occur when $C^* > C_{11}^*$. The influence of C^* on C'_f and C'_m is similar to that for longitudinal excitations. No resonances are possible if $H/T < 1668$ ft/sec for $b^* = 2.0$. A low dam design is safer.
- (3) The hydrodynamic pressure generally increases towards the base, especially when $C^* < C_{11}^*$. However, oscillations may occur when $C^* > C_{11}^*$. A bending reinforcement for a dam is also important.

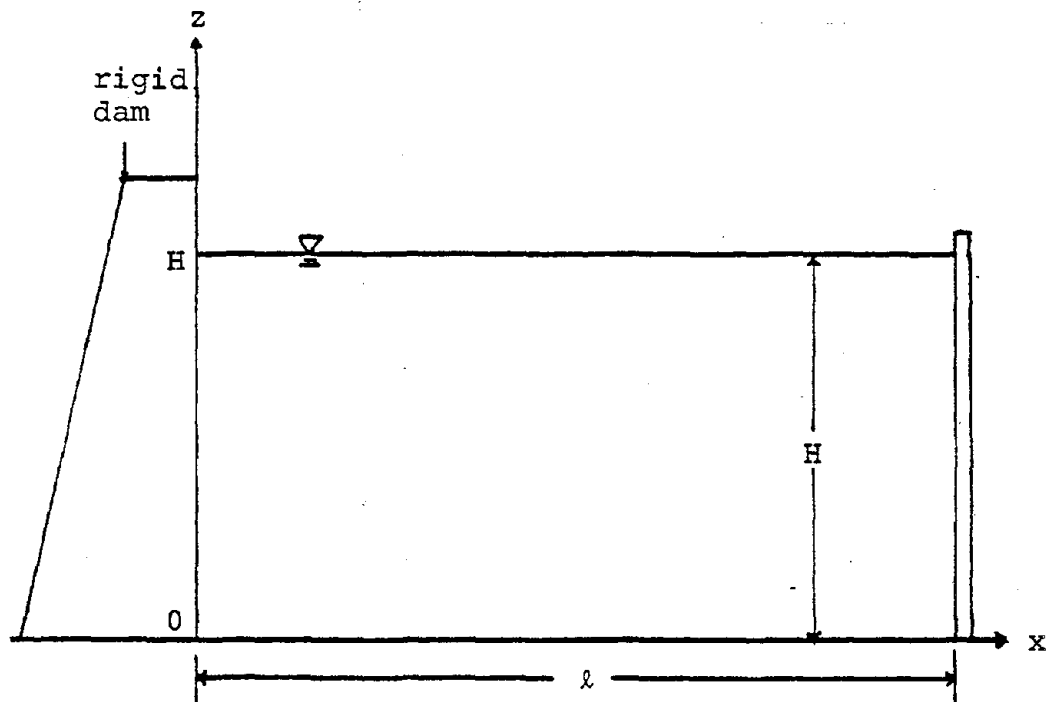
This thesis presents analytic solutions for the problem of earthquake effect on a three-dimensional dam-reservoir system. The effects of seismic wave attenuation and phase change along the longitudinal direction of the reservoir are also included.

Bustamante et al. (1966) concluded that the error introduced by ignoring the surface waves is more than 20% if $H/T < 2.6\sqrt{H}$ (H is in meters). Earthquake frequencies are random in character and spread over a wide range. It follows that for $T > 3$ sec, surface wave effects should not be neglected.

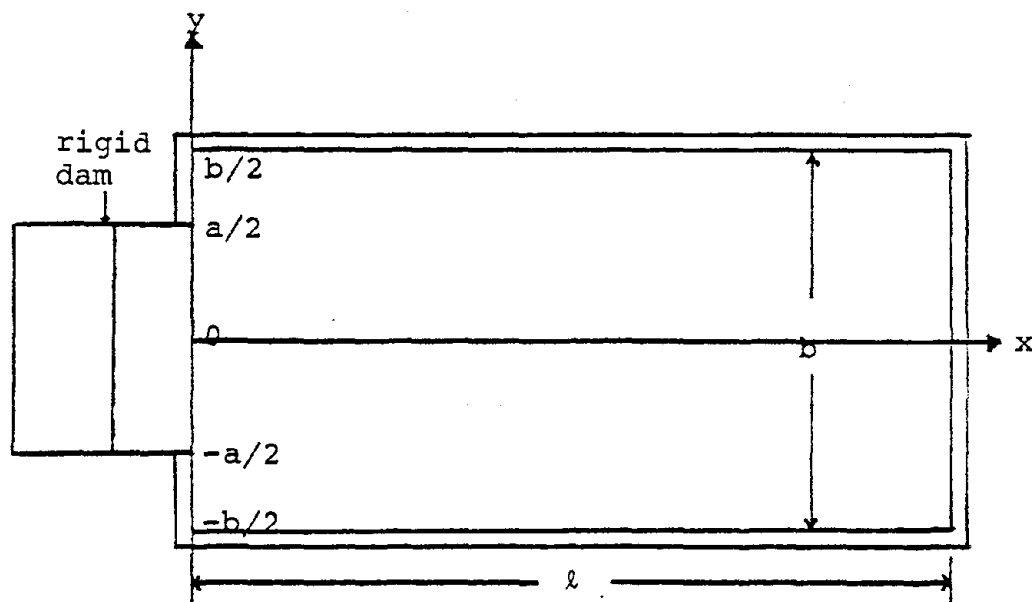
The dam is assumed to be rigid in this thesis. However, the fundamental natural frequency of the dam may be close to the excitation frequencies of an earthquake, therefore the interaction between the reservoir and the flexible dam should be studied.

REFERENCES

- Bustamante, J.I., and Flores, A., 1966, "Water Pressures on Dams Subjected to Earthquakes", J. Eng. Mech. Division, ASCE, 92, 115-127.
- Chopra, A.K., 1967, "Hydrodynamic Pressures on Dams during Earthquakes", J. Eng. Mech. Division, ASCE, 93, 205-223.
- Chwang, A.T., 1978, "Hydrodynamic Pressures on Sloping Dams during Earthquakes. Part 2. Exact Theory", J. Fluid Mech., 87, 343-348.
- Knopoff, L., 1964, Review of Geophysics, 2, 625-660.
- Kotsubo, S., 1959, "Dynamic Water Pressure on Dams due to Irregular Earthquakes", Memoirs Faculty of Engineering, Kyushu University, Fukuoka, Japan, 18, 119-129.
- Press, F., 1964, "Seismic Wave Attenuation in the Crust", J. Geophy. Reseach, 69, 4417-4418.
- Werner, P.W., and Sundquist, K.J., 1949, "On Hydrodynamic Earthquake Effects", Transactions, American Geophysical Union, 30, 636-657.
- Westergaard, H.M., 1933, "Water Pressures on Dams during Earthquakes", Transactions, ASCE, 98, 418-433.
- Zangar, C.N., 1953, "Hydrodynamic Pressures on Dams due to Horizontal Earthquakes", Monograph No. 11, Proc. Soc. Ex. Stress Analo., 10, 93-102.

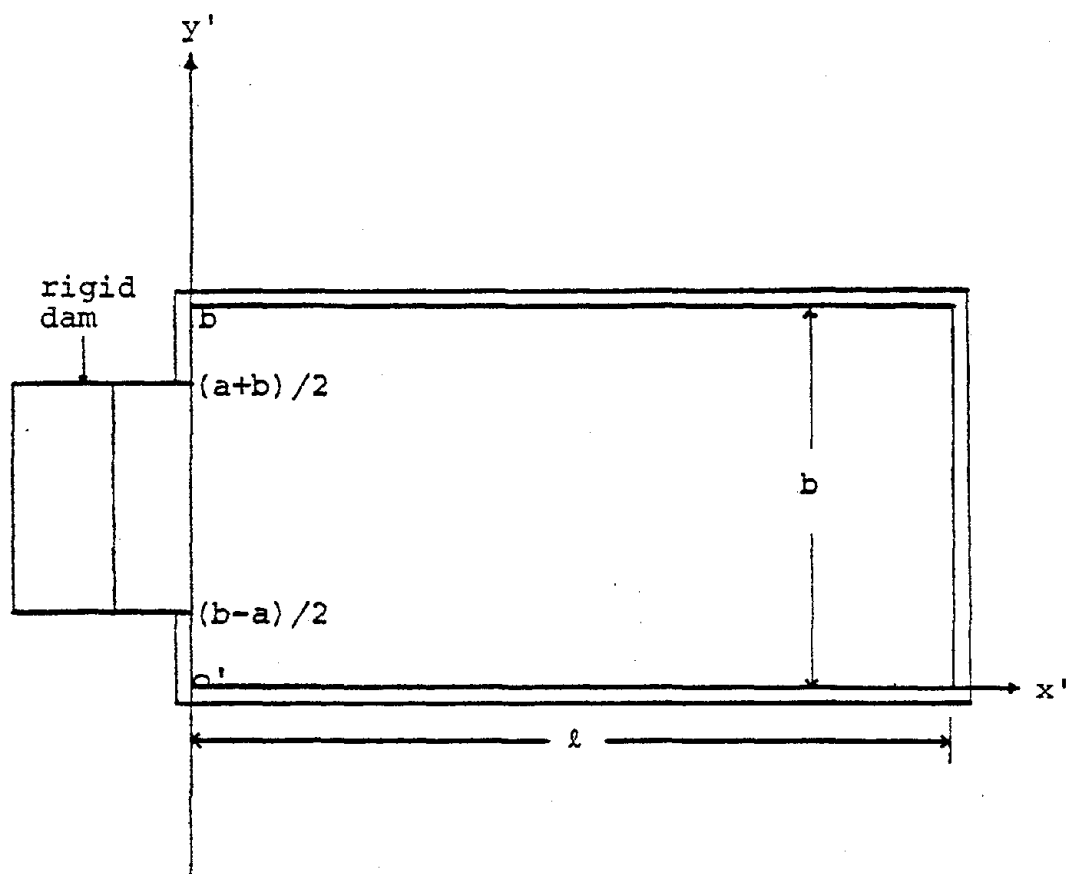


(a) Side View



(b) Top View

Figure 1. A Schematic Diagram of a Rectangular Dam-Reservoir System



(c) $x'y'z'$ Coordinate System

Figure 1. (cont'd)

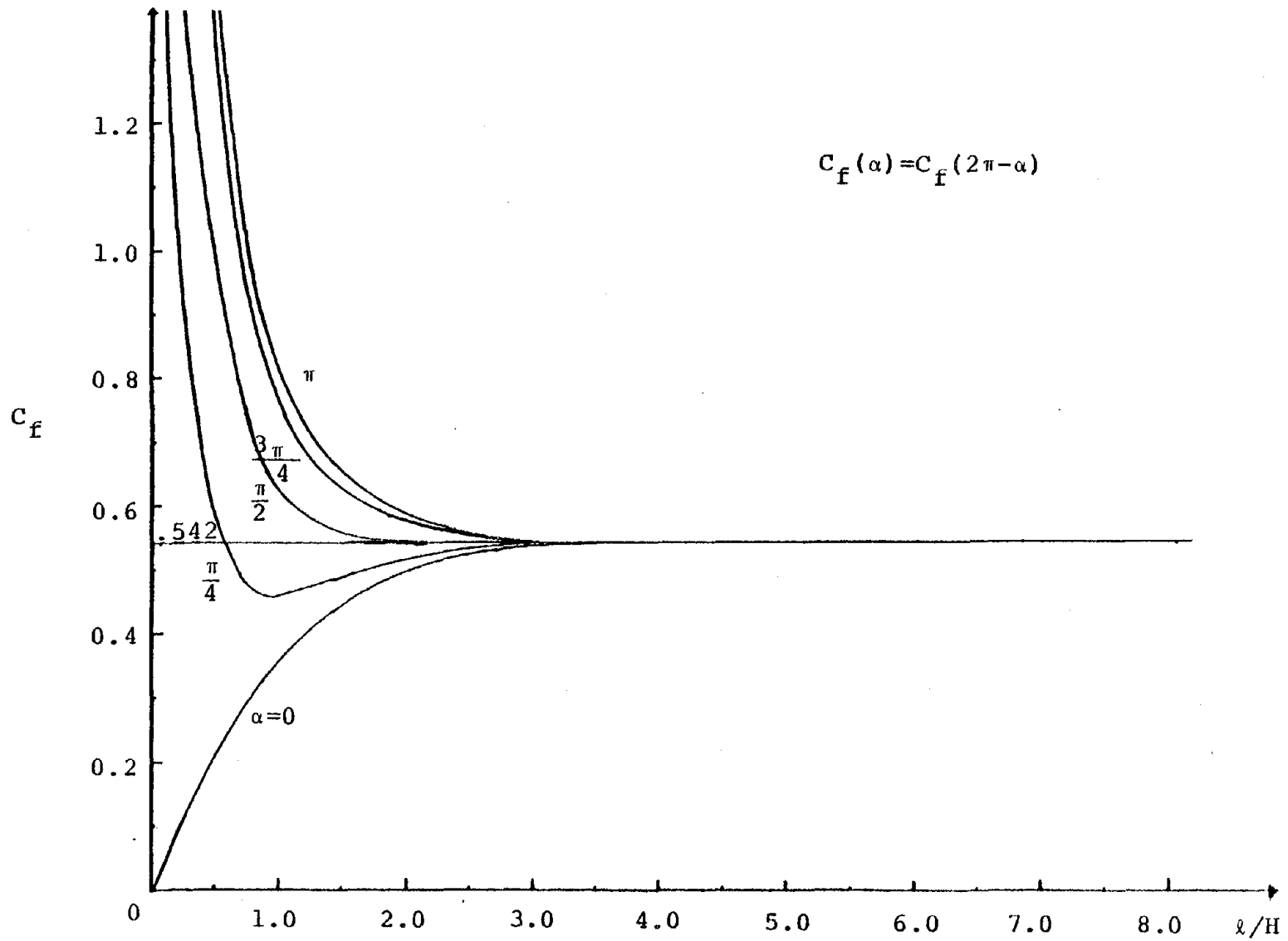


Figure 2. Variation of the Hydrodynamic Force Coefficient with the Length-to-Depth Ratio l/H due to a Longitudinal Excitation at $\beta=1.0$ and $\omega H/c=0.0$

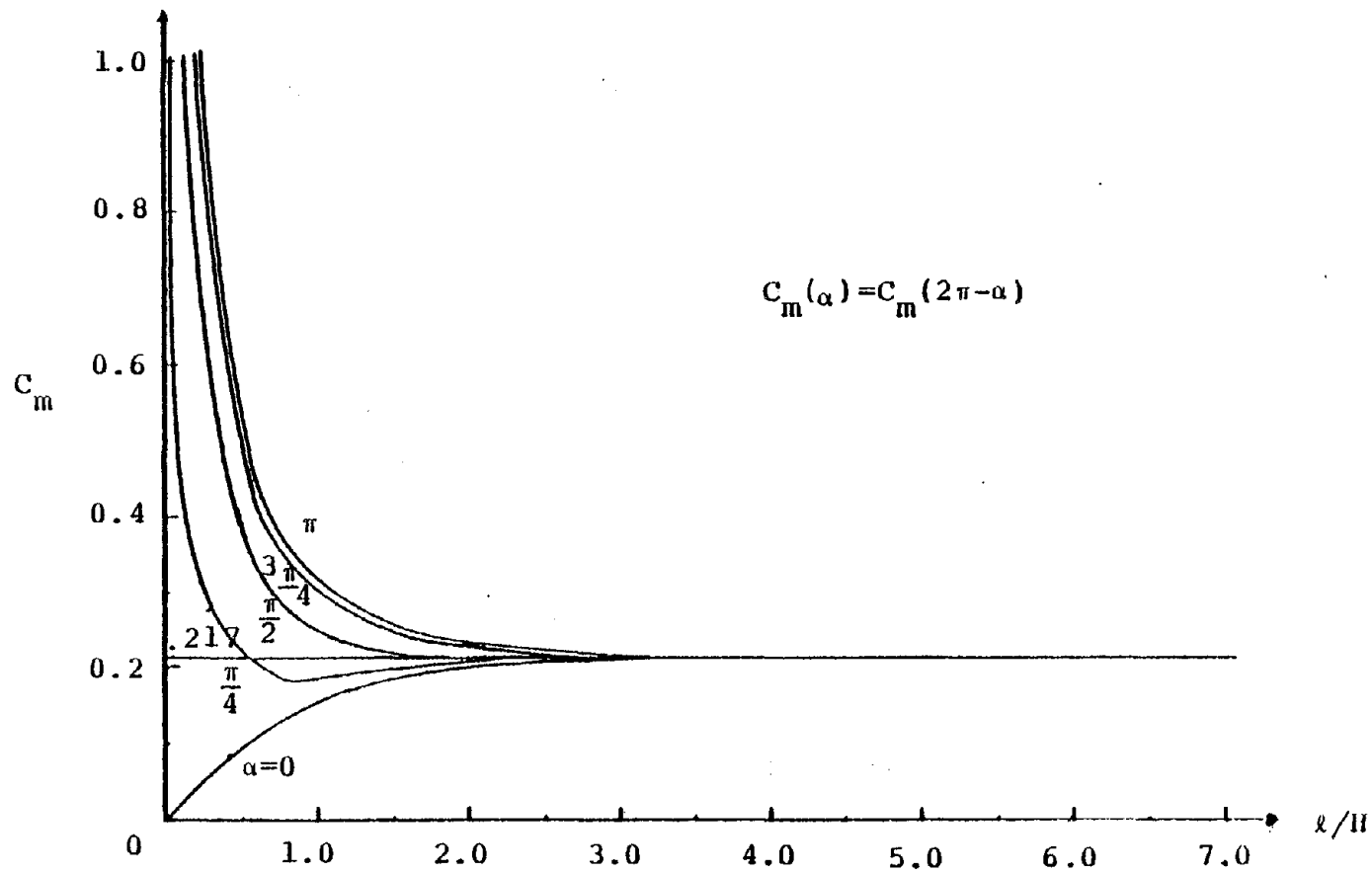


Figure 3. Variation of the Hydrodynamic Moment Coefficient with the Length-to-Depth Ratio l/H due to a Longitudinal Excitation at $\beta=1.0$ and $\omega H/c=0.0$

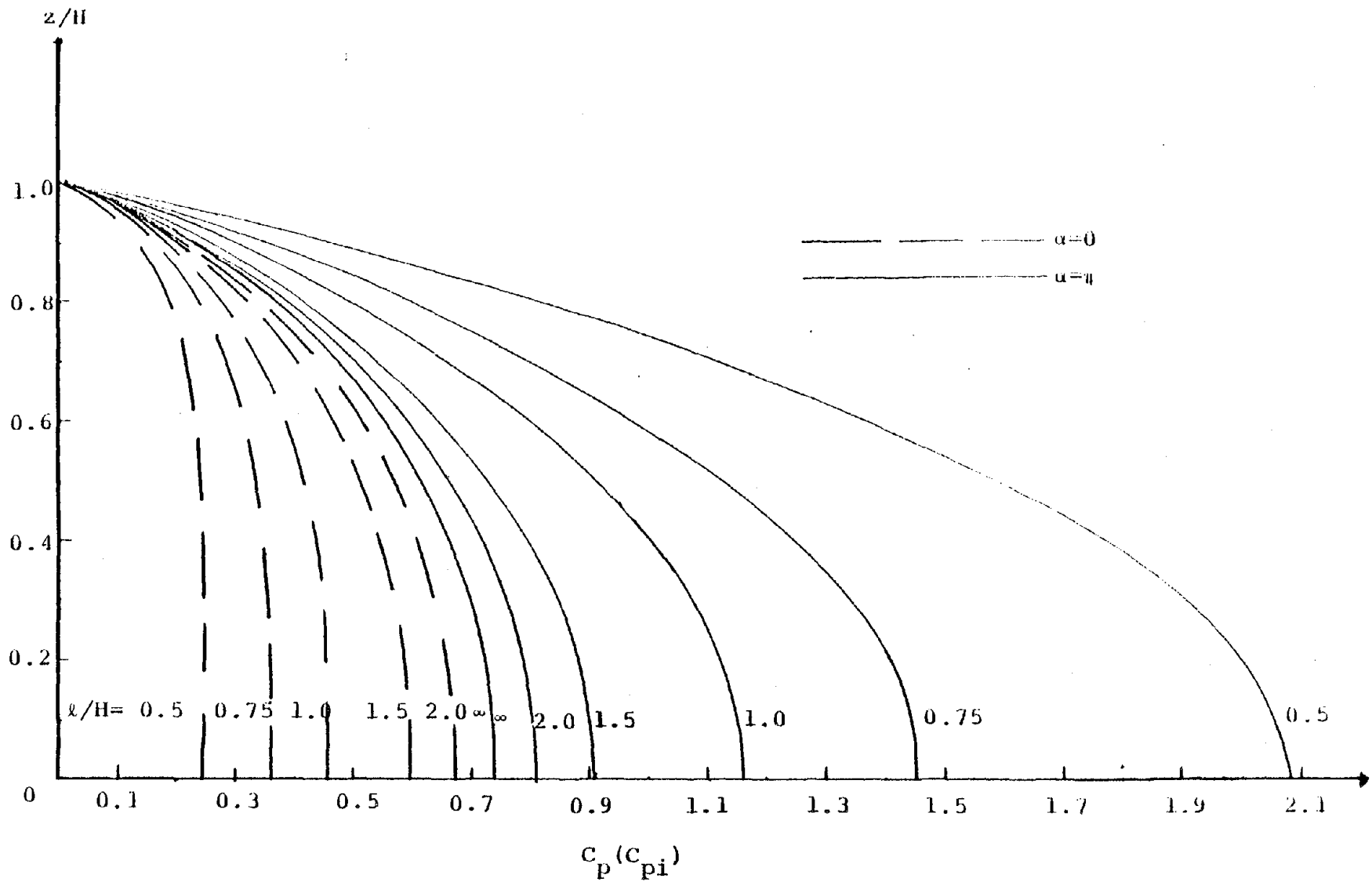


Figure 4. Variation of the Hydrodynamic Pressure Coefficient with the length-to-Depth Ratio λ/H due to a Longitudinal Excitation at $\beta=1.0$, $\omega H/c=0.0$, $\alpha=0$, and $\alpha=\pi$

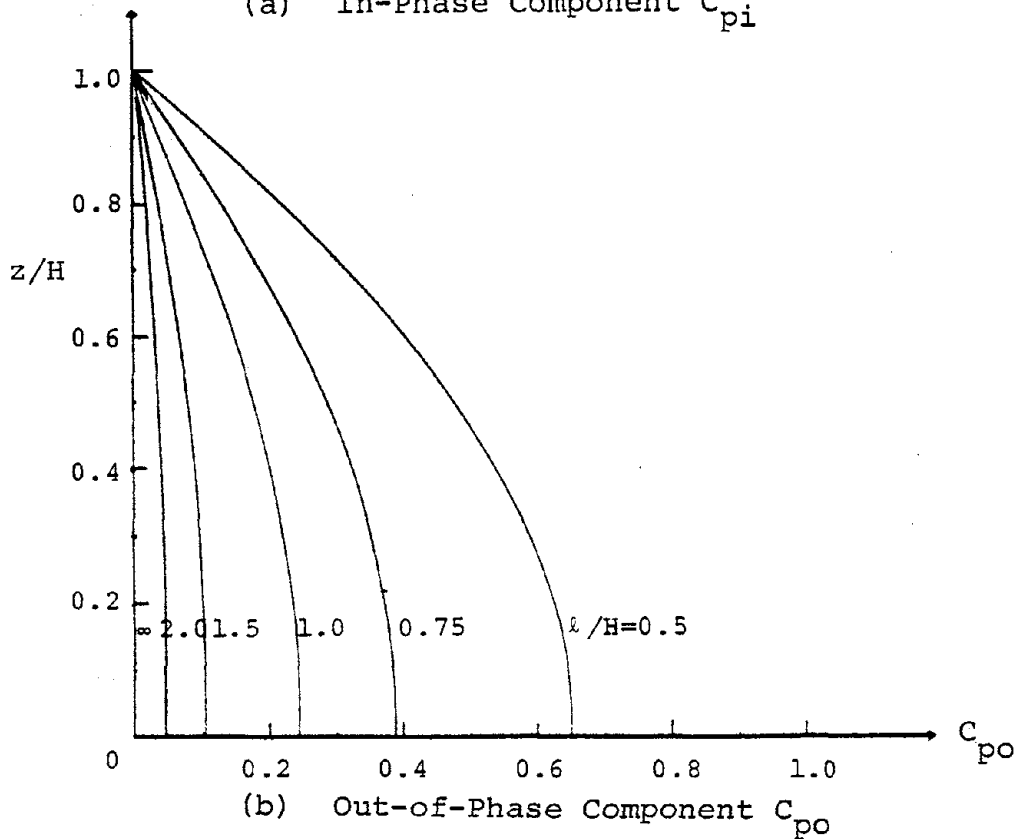
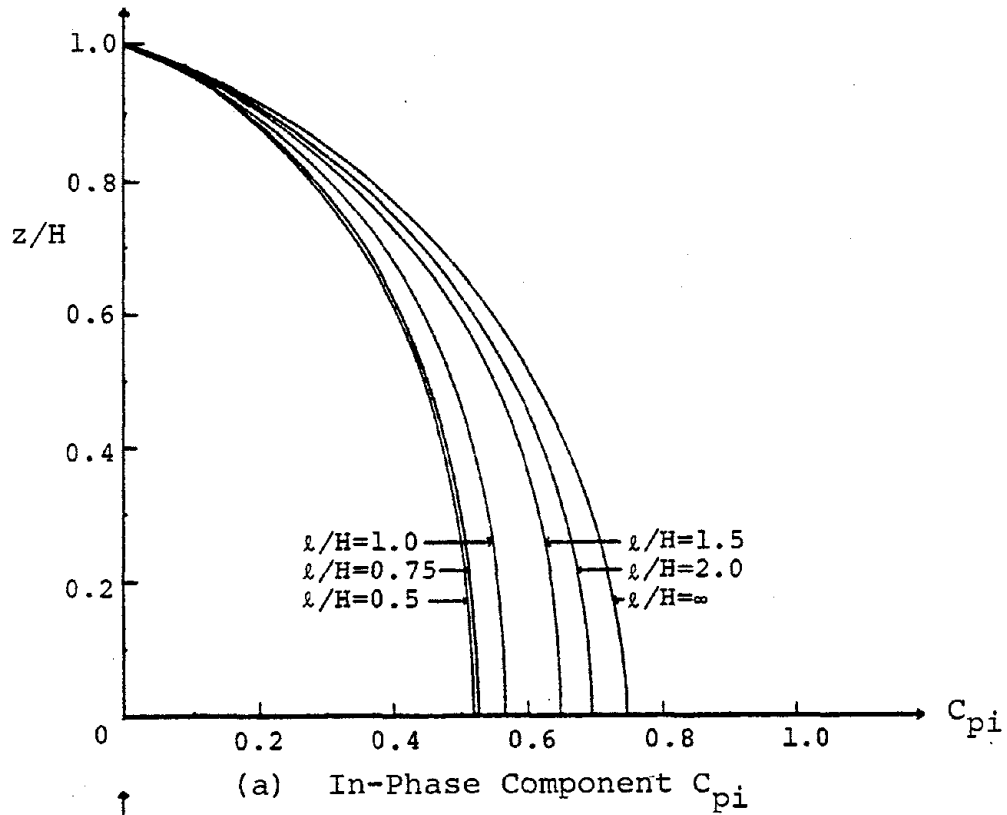
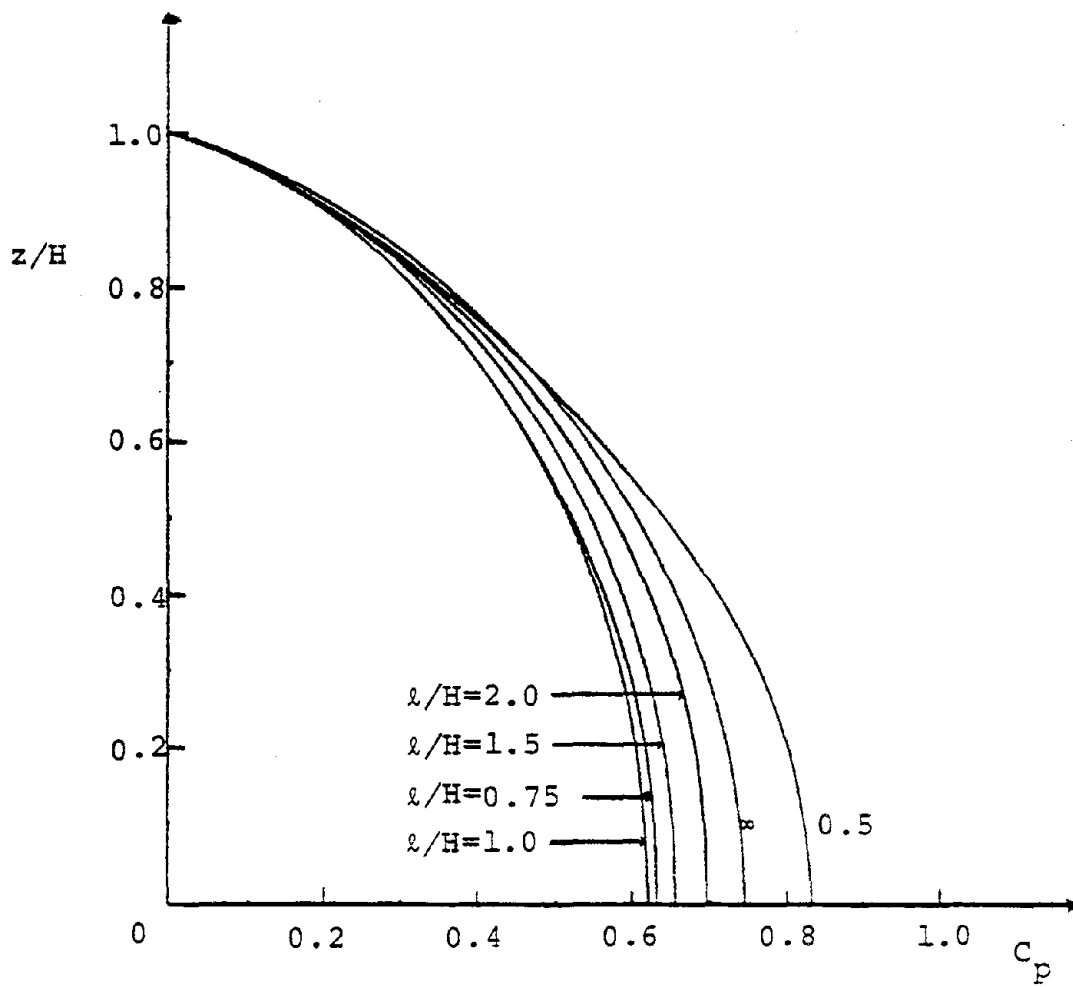


Figure 5. Variation of the Hydrodynamic Pressure Coefficient with the Length-to-Depth Ratio λ/H due to a Longitudinal Excitation at $\beta=1.0$, $\omega H/c=0.0$, and $\alpha=\pi/4$



(c) Total Hydrodynamic Pressure Coefficient C_p

Figure 5. (cont'd)

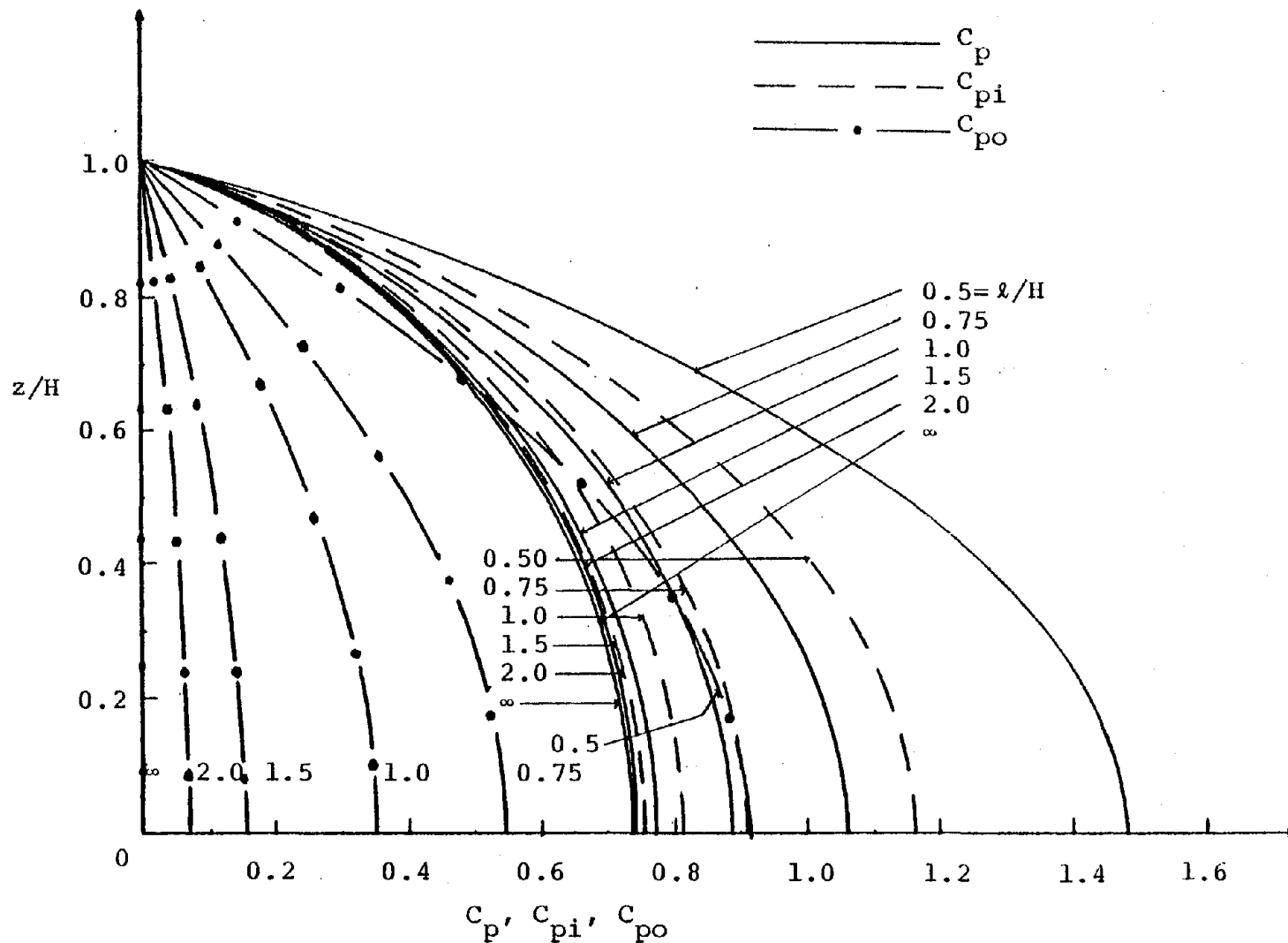


Figure 6. Variation of the Hydrodynamic Pressure Coefficient with the Length-to-Depth Ratio l/H due to a Longitudinal Excitation at $\beta=1.0$, $\omega H/c=0.0$, and $\alpha=\pi/2$

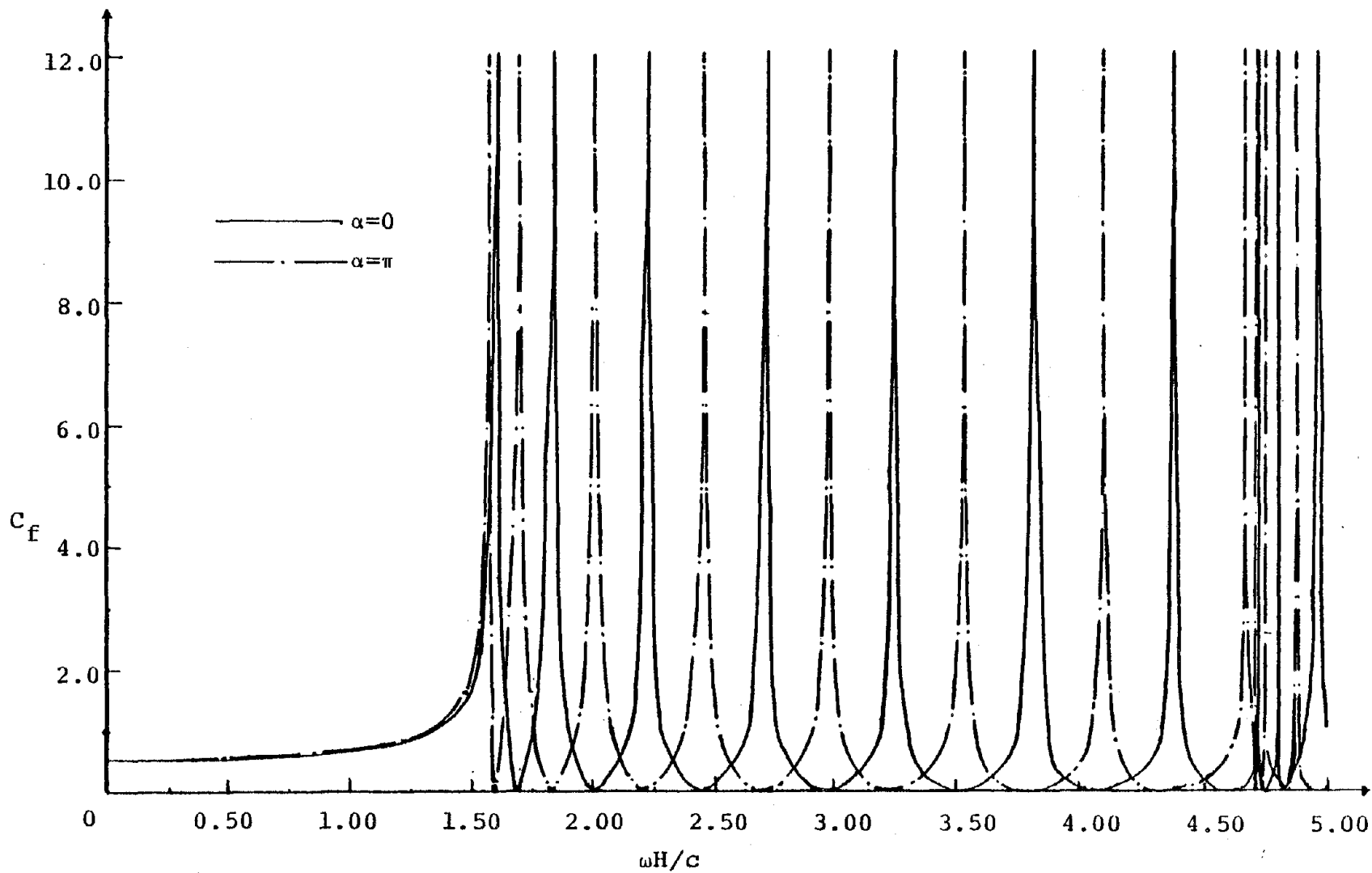


Figure 7. Variation of the Hydrodynamic Force Coefficient with the Compressibility Parameter $\omega H/c$ due to a Longitudinal Excitation at $\beta=1.0$, $\epsilon/H=10.0$, $\alpha=0$, and $\alpha=\pi$

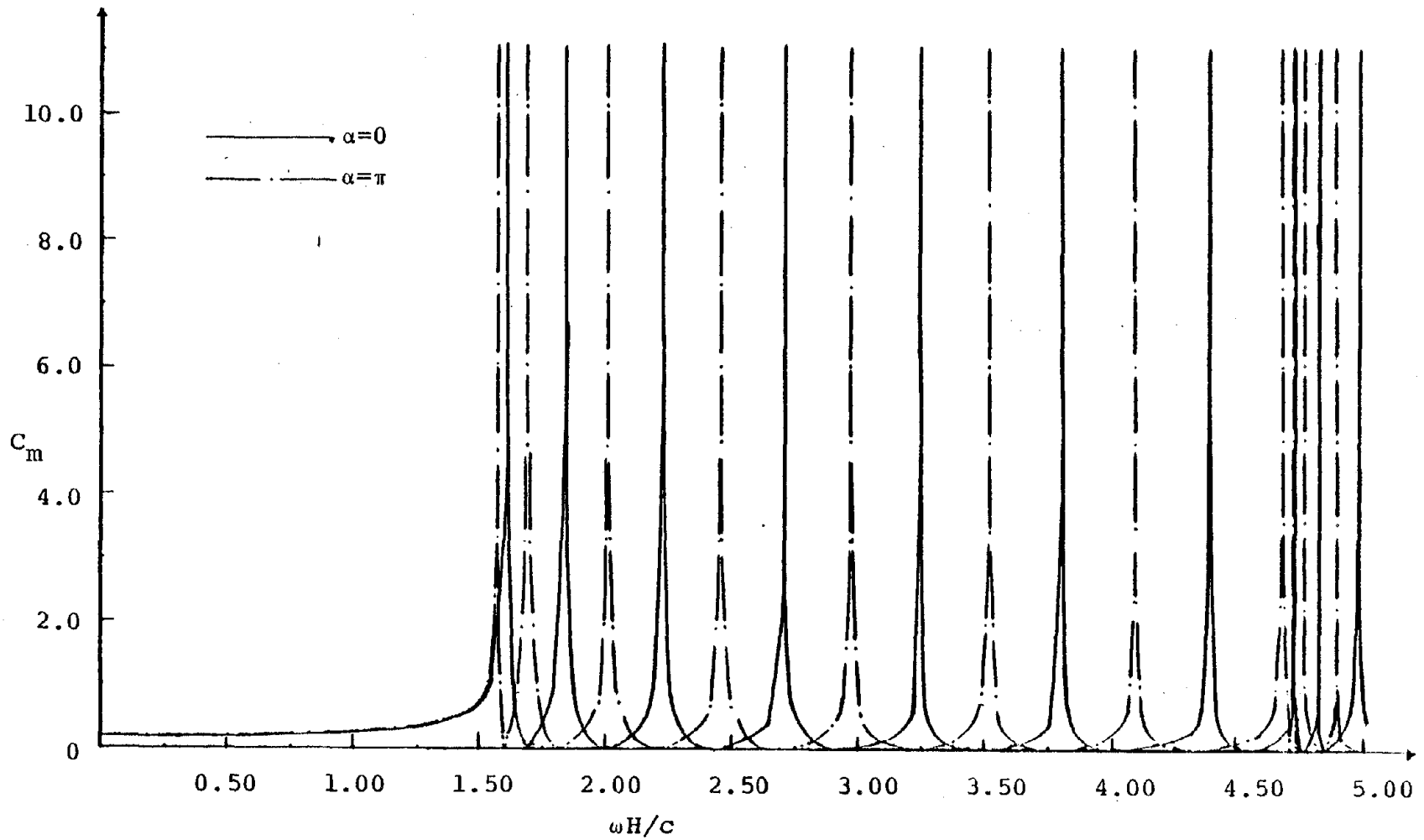


Figure 8. Variation of the Hydrodynamic Moment Coefficient with the Compressibility Parameter $\omega H/c$ due to a Longitudinal Excitation at $\beta=1.0$, $l/H=10.0$, $\alpha=0$, and $\alpha=\pi$

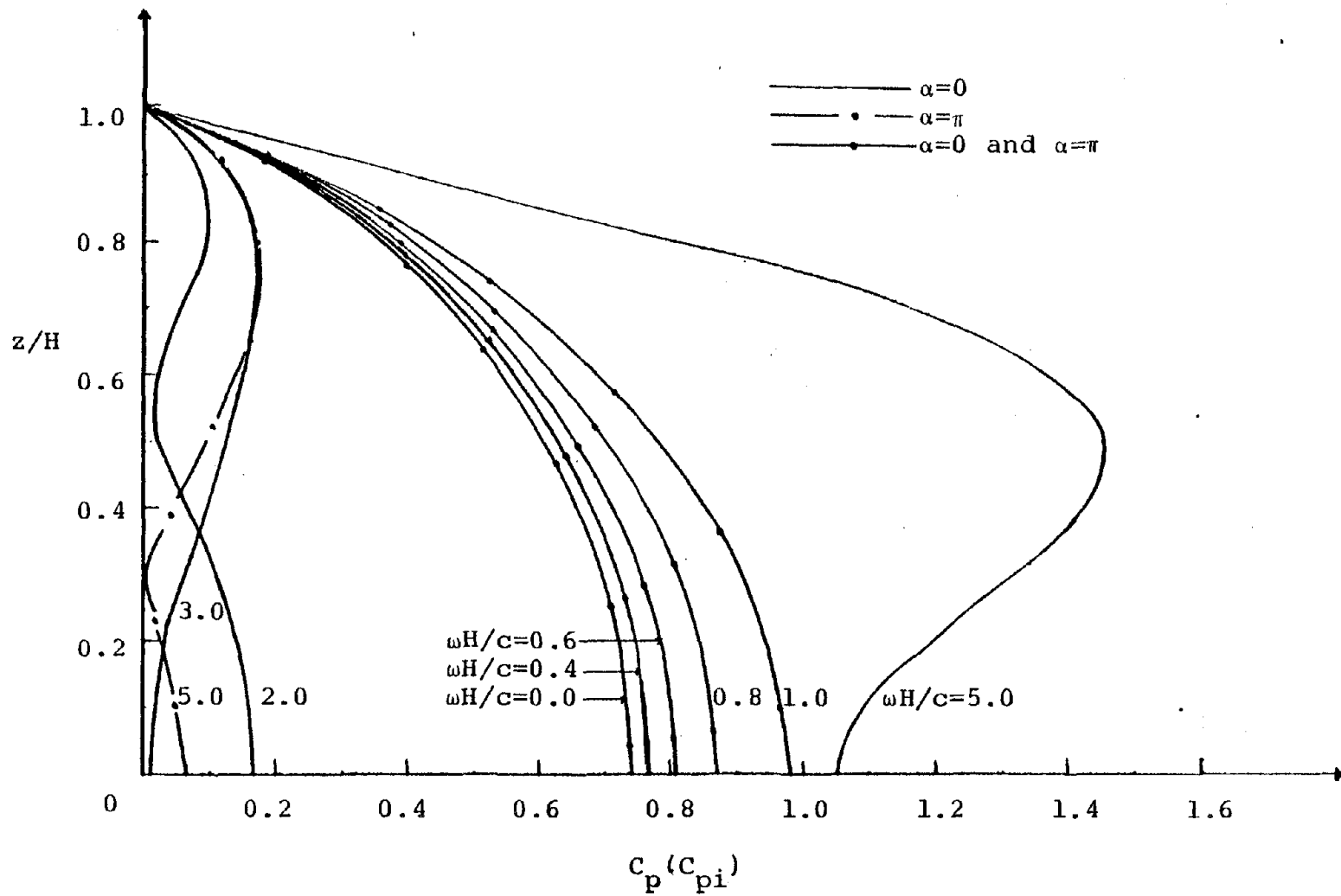


Figure 9. Variation of the Hydrodynamic Pressure Coefficient with the Compressibility Parameter $\omega H/c$ due to a Longitudinal Excitation at $\beta=1.0$, $l/H=10.0$, $\alpha=0$, and $\alpha=\pi$

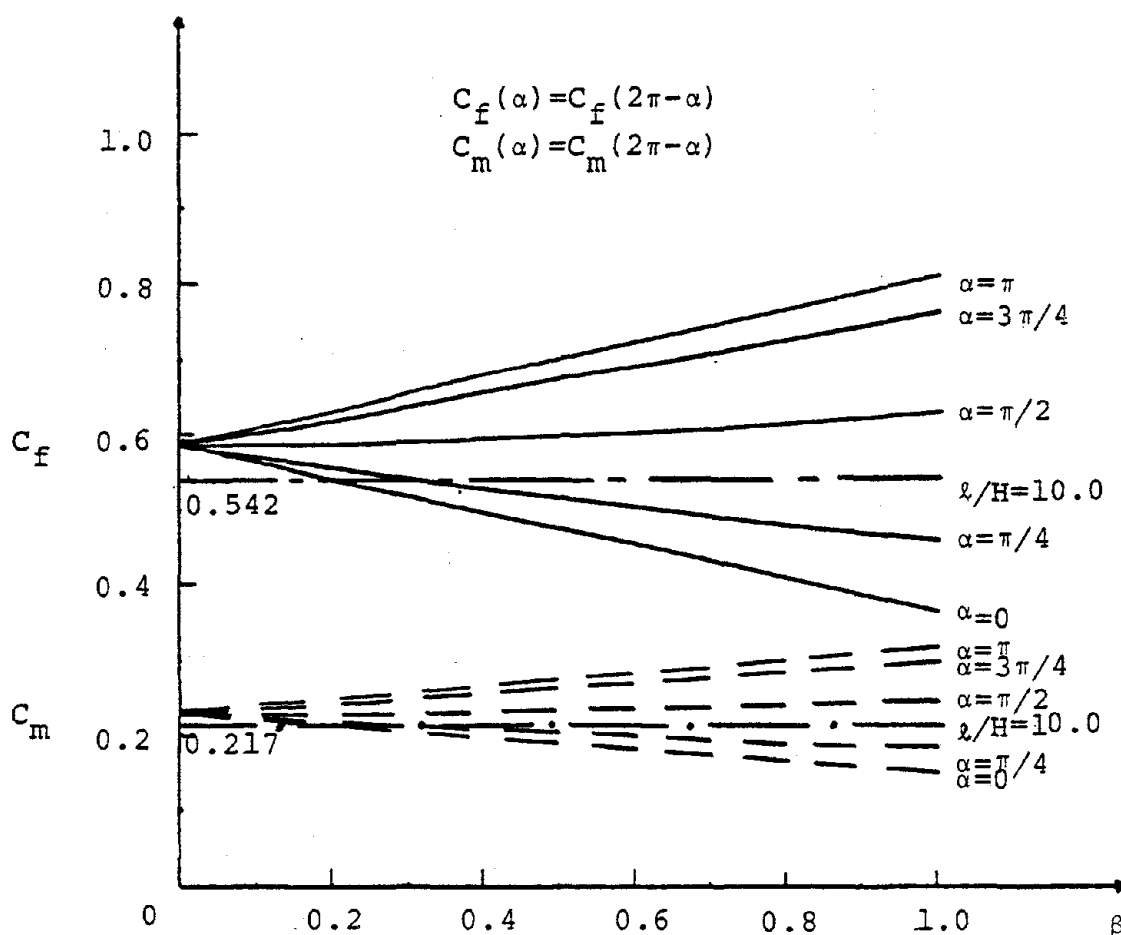


Figure 10. Variation of the Hydrodynamic Force and Moment Coefficients with the Attenuation Factor β due to a Longitudinal Excitation at $\omega H/c=0.0$, $\lambda/H=1.0$, and $\lambda/H=10.0$

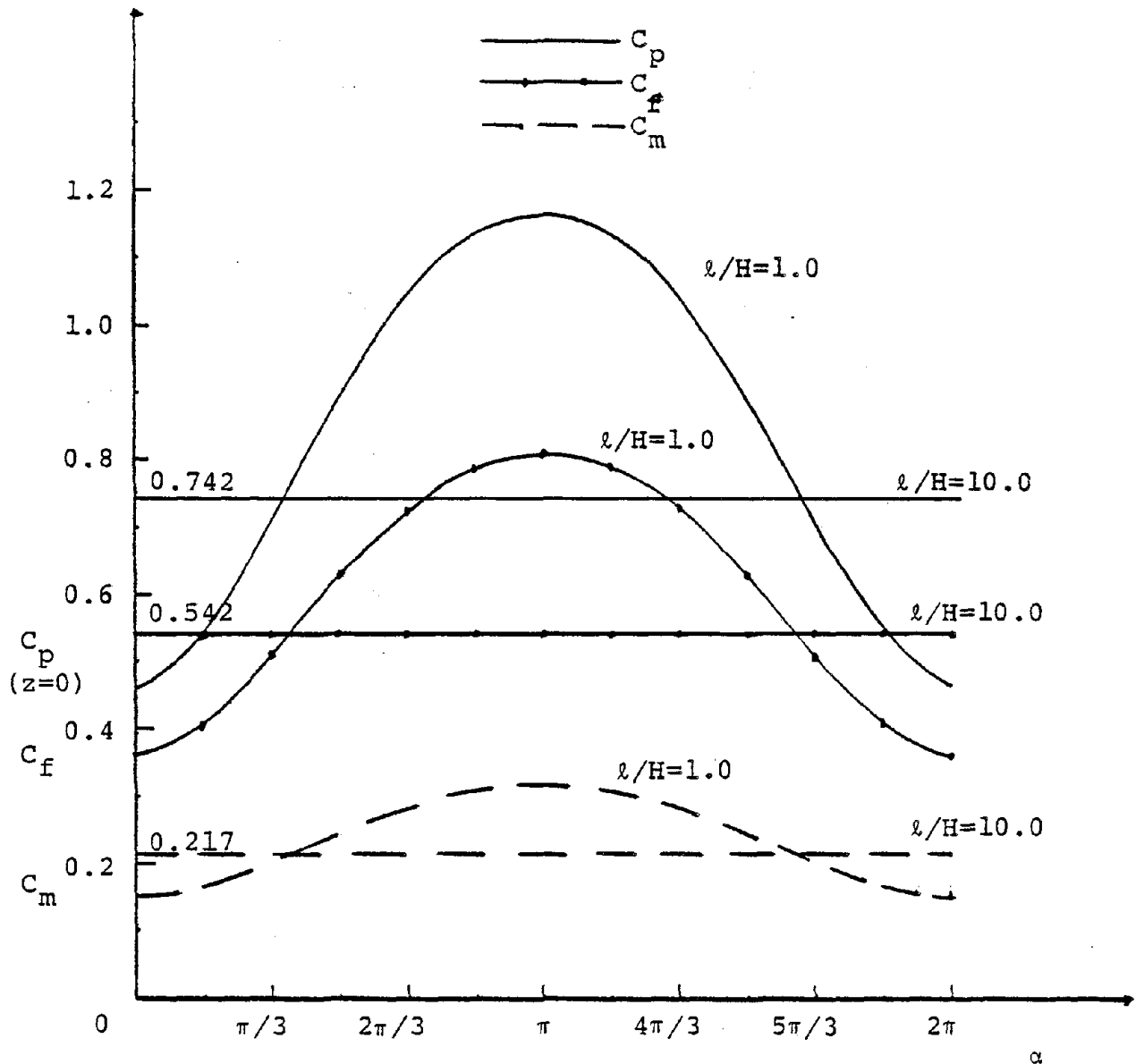


Figure 11. Variation of the Hydrodynamic Pressure, Force, and Moment Coefficients with the Phase-Shift Angle α due to a Longitudinal Excitation at $\beta=1.0$, $\omega H/c=0.0$, $l/H=1.0$, and $l/H=10.0$

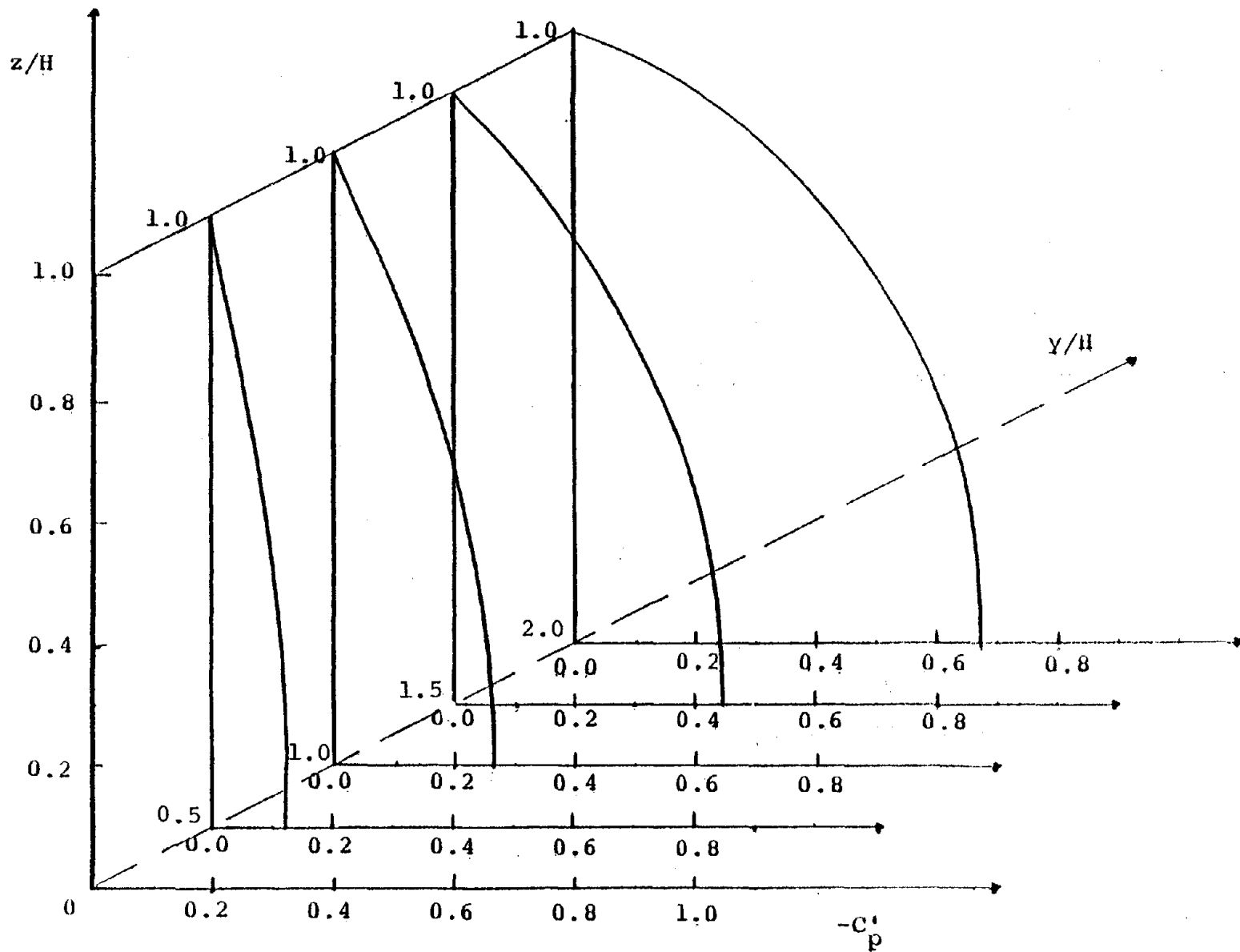


Figure 12. Variation of the Hydrodynamic Pressure Coefficient with the Width-to-Depth Ratio y/H due to a Lateral Excitation at $\omega H/c=0.0$ and $b/H=2.0$

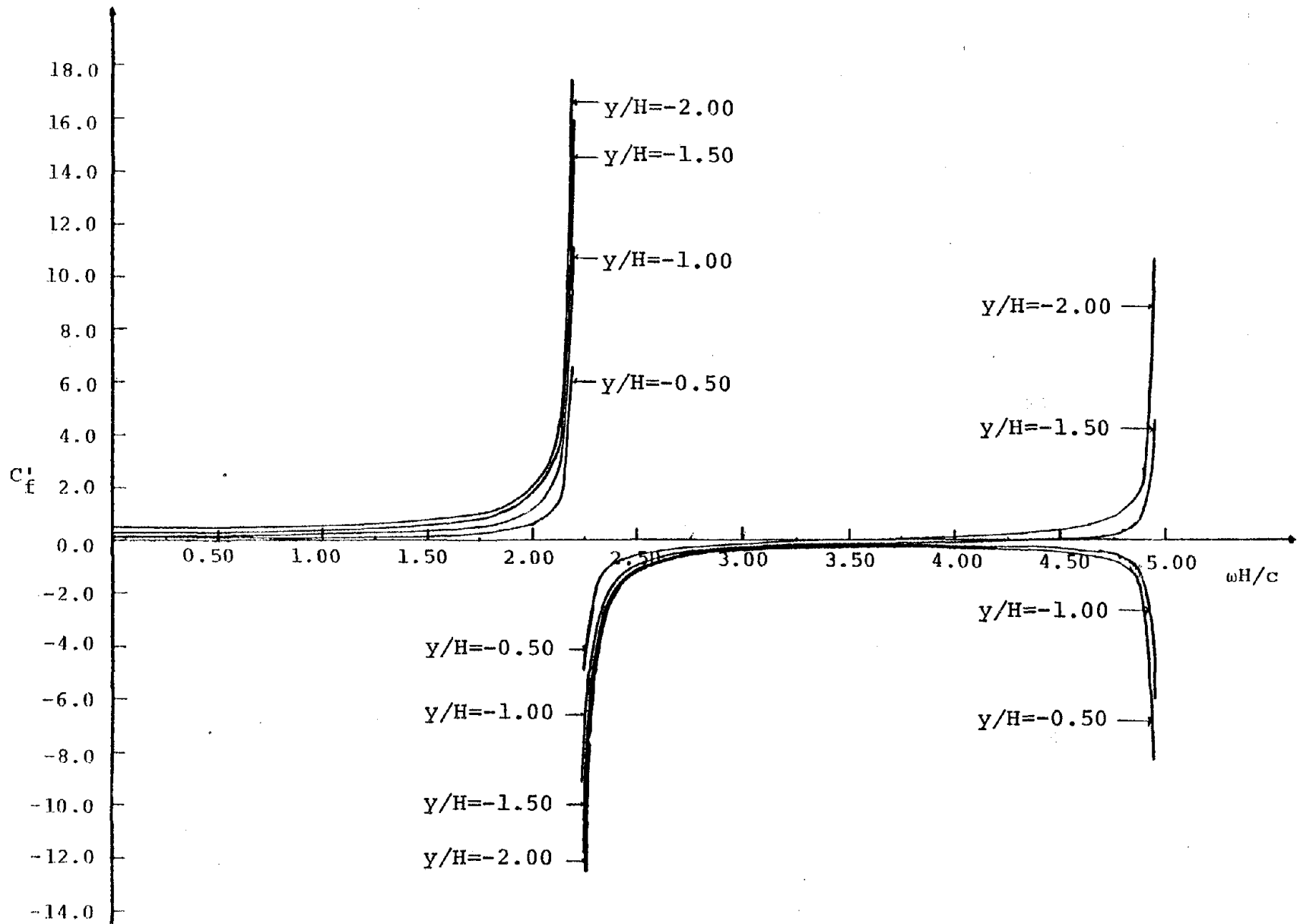


Figure 13. Variation of the Hydrodynamic Force Coefficient with the Compressibility Parameter $\omega H/c$ due to a Lateral Excitation at $b/H=2.0$ and $a/b=1.0$

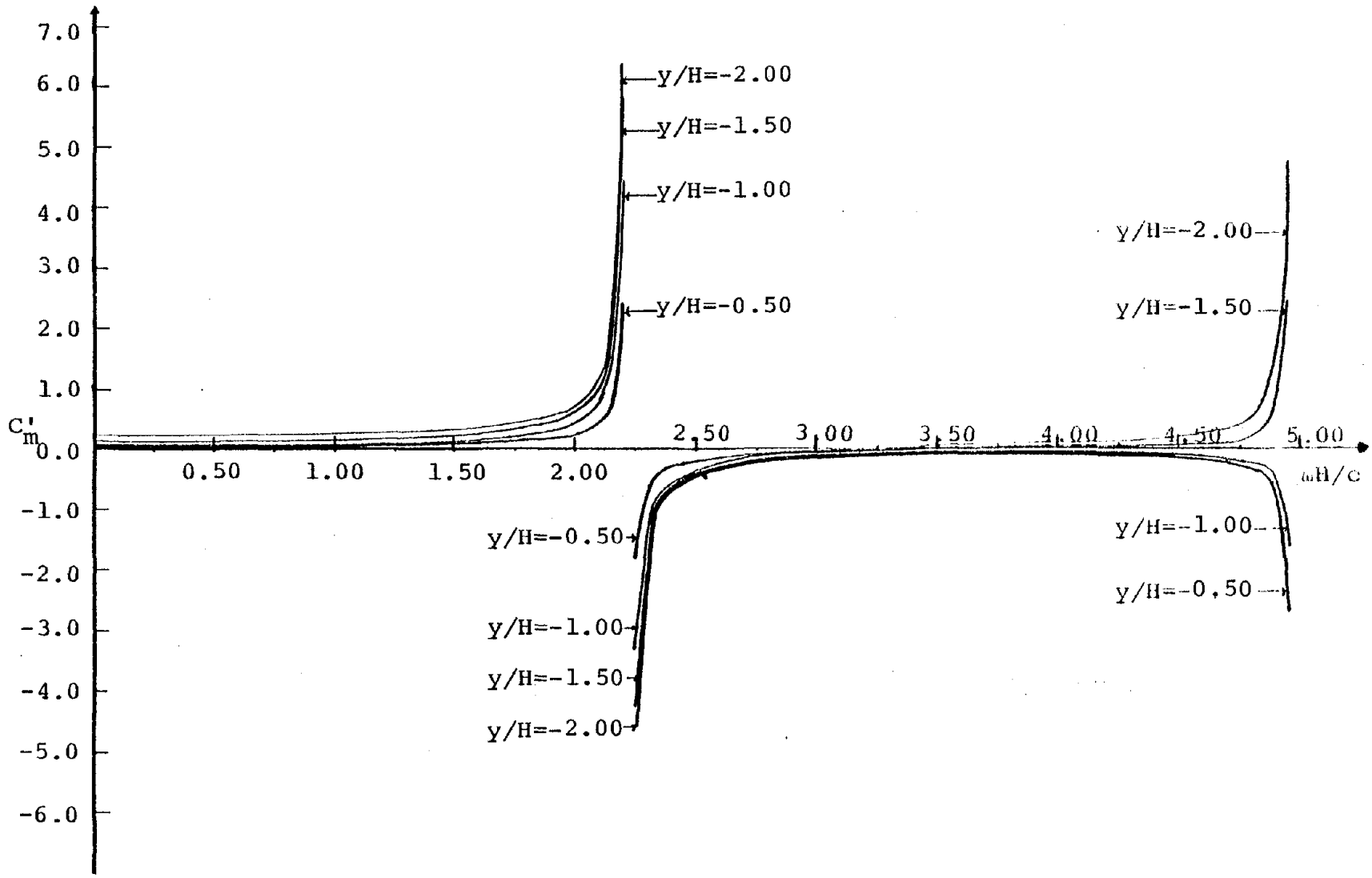


Figure 14. Variation of the Hydrodynamic Moment Coefficient with the Compressibility Parameter $\omega H/c$ due to a Lateral Excitation at $b/H=2.0$ and $a/b=1.0$

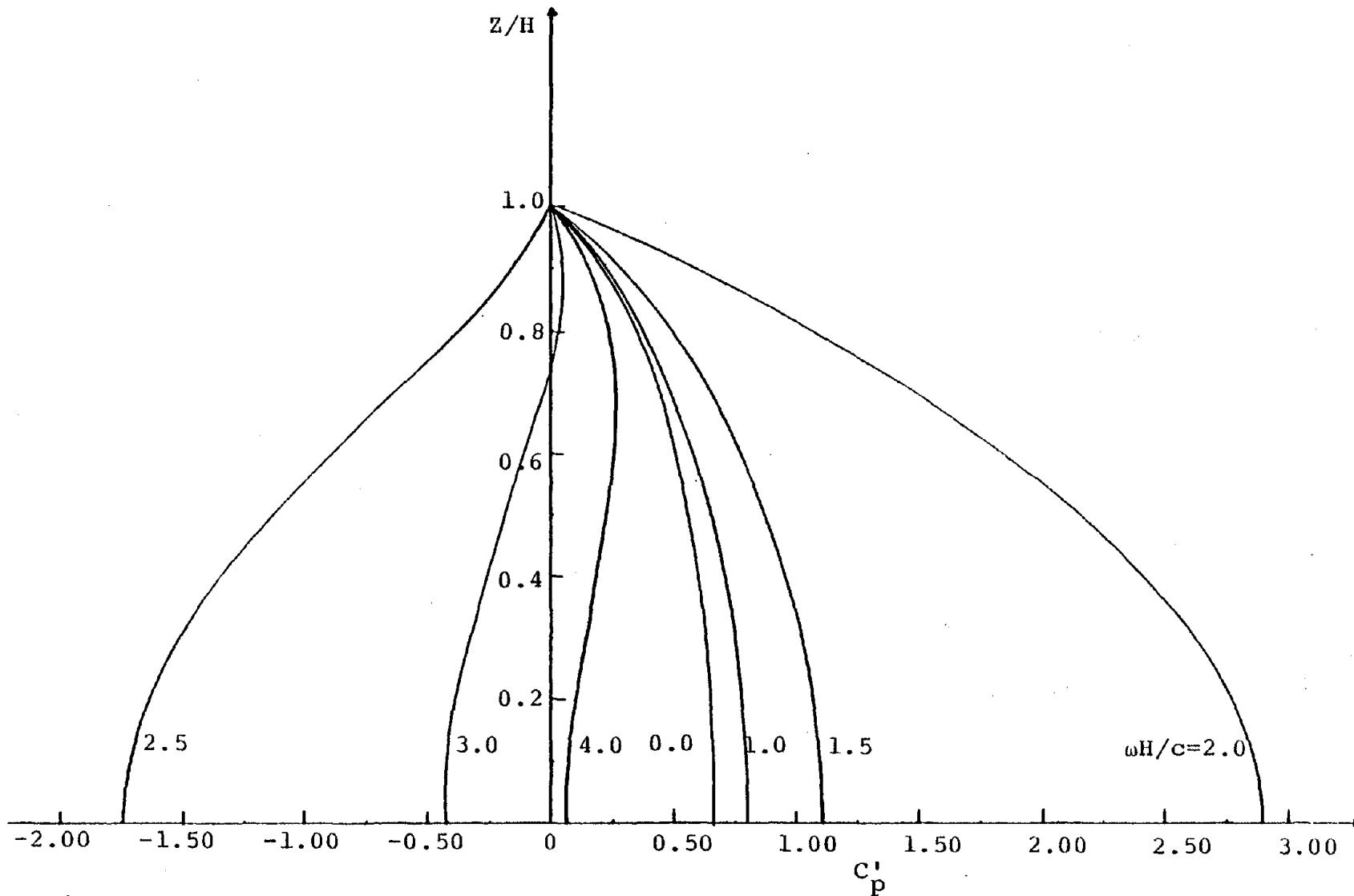


Figure 15. Variation of the Hydrodynamic Pressure Coefficient with the Compressibility Parameter $\omega H/c$ due to a Lateral Excitation at $b/H=2.0$, $a/b=1.0$, and $y/H=-1.0$